Enhancing extraordinary magnetoresistance devices through geometric variations of the outer boundary

Pomar, Thierry Désiré; Frąckowiak, Adrianna Elżbieta; Erlandsen, Ricci; Christensen, Dennis Valbjørn; Bjørk, Rasmus

Published in:
Journal of Applied Physics

Link to article, DOI:
10.1063/5.0154997

Publication date:
2023

Document Version
Peer reviewed version

Enhancing Extraordinary Magnetoresistance Devices Through Geometric Variations of the Outer Boundary

Thierry Désiré Pomar*, Adrianna Elżbieta Frackowiak, Ricci Erlandsen, Dennis Valbjørn Christensen, Rasmus Bjørk*

Department of Energy Conversion and Storage, Technical University of Denmark - DTU, Anker Engelunds Vej 1, DK-2800 Kgs. Lyngby, Denmark

Abstract

Magnetometers with a high sensitivity at weak magnetic fields are desirable for a wide range of sensing applications. Devices which operate on the principle of extraordinary magnetoresistance (EMR) are appealing candidates because of their simplicity and ability to operate at room temperature but they suffer from low sensitivity when compared to state-of-the-art magnetometers such as superconducting quantum interference devices (SQUIDs). Since the EMR phenomenon is principally a geometric effect, the shapes of the various parts of the device represent additional degrees-of-freedom which can be manipulated in order to modify the performance of the devices. While previous studies have mostly focused on the inner part of the sensor, in this work we study the effect of systematically manipulating the shape of the outer boundary. We show that the maximum sensitivity of the device can be increased by 70% by placing a constriction between the voltage or current probes and by 300% if the shape of the boundary is shifted from circular to elliptical. We also show that a finite zero-field sensitivity can be obtained if the horizontal symmetry of the device is broken. These results demonstrate that the outer boundary can have a significant effect on device performance, a finding which paves the way for using shape optimization on the outer boundary for designing sensitive magnetometers.

1. Introduction

Magnetoresistance is a property of some material systems wherein the measured electrical resistance changes as a function of applied magnetic field. There are many phenomena which produce the effect, though they can be separated into two general categories: physical magnetoresistance which occurs as a consequence of material properties, and geometric magnetoresistance which arises from the interaction between charge carriers and the device geometry.[1] Physical magnetoresistance can emerge out of a variety of different material behaviors. For example, metals typically display a small positive magnetoresistance as the trajectory of charge carriers in a magnetic field is deflected by the Lorentz force, resulting in an increased path length and a subsequently higher resistance. Spin-orbit interactions between electrons and atomic orbitals produce an anisotropic magnetoresistance (AMR) in ferromagnetic materials and giant magnetoresistance (GMR) in alternating ferromagnetic and non-magnetic thin film heterostructures. The quantum mechanical nature of charge carriers can also produce physical magnetoresistance. The magnitude of the change in resistance can vary from quite small, in the range of a few percent for common magnetoresistance, to up to several hundred percent for GMR devices.[2, 3]

As with conventional magnetoresistance observed in metals, geometric magnetoresistance is also caused by the Lorentz force but is primarily driven by the boundary conditions around the current flow. This so-called extraordinary magnetoresistance (EMR) effect can be observed in hybrid devices formed from high mobility semiconductors embedded with highly conductive inhomogeneities. [4] In the absence of a magnetic field current flows preferentially through the conductive material, effectively

*Corresponding author
Email addresses: thipom@dtu.dk (Thierry Désiré Pomar), rabj@dtu.dk (Rasmus Bjørk)

shorting the circuit and producing a low resistance. If subjected to a magnetic field oriented perpendicular to the plane of the device however, the current is deflected around the conductive material and forced to travel through the relatively high resistance semiconductor material instead. The deflection of the current occurs if the contrast in the conductivity between the two materials is large enough that the conductive inhomogeneity essentially forms an equipotential surface relative to the semiconductor material. Under this condition, locally the electrical field lines extend radially from the boundary of the inhomogeneity. Charge carriers which approach the boundary experience a Lorentz force perpendicular to the local electrical field, deflecting their orbits along the interface. The Hall angle which determines the magnitude of the deflection depends on both the magnetic field strength and the carrier mobility of the semiconductor material and approaches 90° in the high field limit for both of these parameters, corresponding to a total expulsion of the current from the conductive regions. As the Hall angle increases, a higher percentage of the current is prevented from entering the inhomogeneity, resulting in a device whose measured resistance varies as a function of the applied magnetic field.

A simple form of the effect can be observed in Corbino discs, which are devices where the outer perimeter forms a grounded contact and a second contact in the center of the device is used to inject a current.[5] In the absence of a magnetic field the current flows radially, but once a field is applied the Lorentz force causes the current path to spiral. The magnitude of the deflection is determined by the magnetic field strength and the carrier mobility of the material. For high mobility materials, these resistance changes can be up to several thousand percent in strong magnetic fields.[6] In the year 2000 a new type of geometric magnetoresistance was described by Solin et al. in semiconductor/metal hybrid devices. These early EMR devices could produce magnetoresistances as high as 750,000% at 8 T, a value large enough to make them obvious candidates for magnetic sensors and switches.[4] The following years have seen a multitude of research efforts emerge which are focused on the production of practical devices which utilize the EMR effect.[7, 8, 9, 10, 11, 12, 13] In the last decade it was shown that extremely high room-temperature mobilities in excess of 140,000 $cm^2V^{-1}s^{-1}$[14] can be achieved in graphene encapsulated between hexagonal boron nitride crystals.[15] In combination with the ability to achieve low carrier densities, this makes graphene a natural candidate for EMR applications. In 2020 Zhou et al. produced devices using encapsulated graphene which reached a record-high magnetoresistance of 10^7% at 8 T [16], a promising result which added another point to the continually expanding frontier of EMR technologies and reinforced the potential for manifesting this effect for practical applications.

Since EMR is a geometric effect in hybrid devices, the shapes of the different material regions can heavily influence the magnetoresistance of the device. Attempts to optimize the geometry of EMR devices in order to improve their performance have mostly been focused on the shape of the metal component.[17, 18, 19] The finite element simulations performed in these studies have found that by modifying the shape of the shunt enormous increases in the magnetoresistance can be achieved: as high as 10^{10}% at 5 T for an InSb/Au device, four orders of magnitude higher than the best case for a concentric circular geometry.[17] However, these enormous magnetoresistances are primarily driven by low zero-field resistances which are obtained by essentially shorting the leads with the metallic inclusion. As a result the low-field sensitivity of these devices is quite poor, more than an order of magnitude lower than that of the concentric geometry with the highest magnetoresistance.[20] Large magnetoresistances are interesting, but a robust sensitivity is necessary for producing magnetometers with a fine field resolution. As such, device designs which can produce both a high magnetoresistance and high weak-field sensitivity are sought. While the effect of modifying the shape of the shunt has been widely explored and documented as described above, the effect of changing the shape of the outer boundary has rarely been elucidated. In this work we examine the behavior of the EMR structure when the shape of the semiconductor portion of the device is systematically deformed, in order to understand if this geometrical parameter can also be used to enhance the performance of these devices with a particular focus on the sensitivity. We do this by using a numerical model which has been shown to match well with experimental results[1, 21] in order to calculate the resistance and sensitivity for EMR devices with different shapes.

1.1. Model Physics

In EMR devices the resistance is typically measured non-locally using four point measurements. Current is injected through one contact and removed through an adjacent grounded contact (see Fig. 1). The two opposite probes are used to measure the electrostatic potential. When measuring the resistance between the two voltage probes, R, the magnetoresistance is defined as:

$$MR(B) = \frac{R(B) - R_0}{R_0} \tag{1}$$

where R_0 is the resistance of the device at a magnetic flux density of $B = 0$ T [3]. The four-point resistance is given by:

$$R(B) = \frac{V_{nl}}{I} \tag{2}$$

where V_{nl} is the potential between the two voltage probes and I is the current supplied to the device.[22] A commonly used metric is the sensitivity, δ, which can be evaluated at a bias magnetic field B_{bias} as:

$$\delta = \left[\frac{dR}{dB}\right]_{B_{bias}} \tag{3}$$

There are two designs which are typically used for EMR sensors: the bar geometry and the van der Pauw (vdP) disc, although the bar design can be shown to be topologically equivalent to a slightly modified vdP disc by using conformal mapping.[23] Though the simple geometry of bar shaped devices makes them better suited for large scale manufacturing, in this study we consider only the vdP geometry which was presented in the original Solin paper.[4].

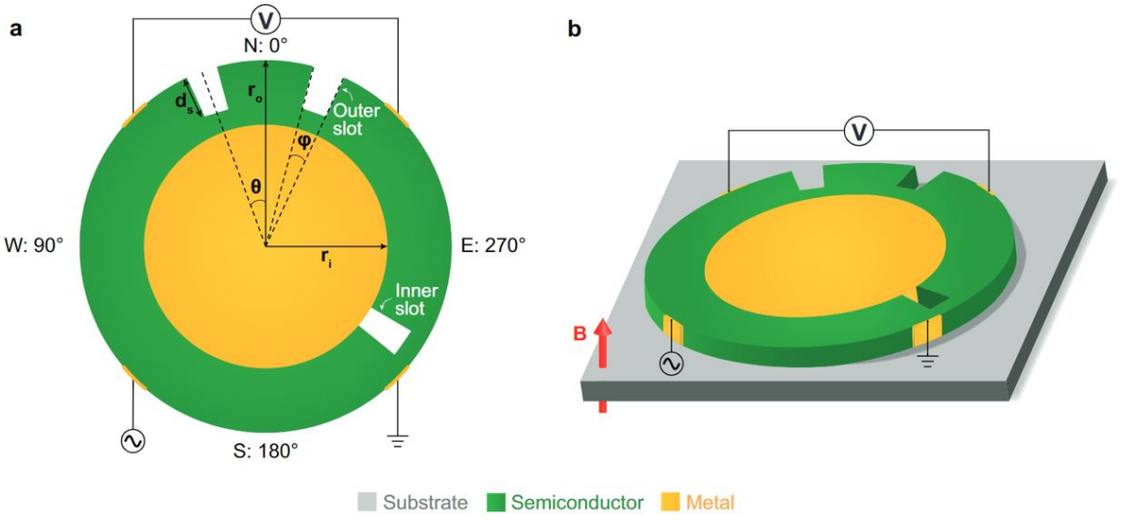

Figure 1: Conceptual figure of the extraordinary magnetoresistive device with slots studied in this work. (a) The various parameters which we use to define the geometry of the sensor and of the deformations to the boundary. (b) A 3D view of the sensor in operation under an applied magnetic field.

Our hypothesis in this work is that EMR device performance can be enhanced by optimizing the geometry of the outer boundary of the semiconductor. First we investigate the effect of modifying the geometry of the system by removing a slot, which consists of an angular section of the semiconductor material as shown in Fig. 1. The location of the slot is given by the angle θ and the width of the slot is

given by its angular span, ϕ. The slot has a depth of d_s as measured from the inner or outer perimeter, depending on which boundary the material is removed from. These two cases are termed an "inner" and "outer" slot, respectively, and both are illustrated in Fig. 1. Finally, in the latter part of this work, we remove the assumption of perfect circularity from the semiconductor portion and examine how the eccentricity of the outer boundary affects the performance of the device.

A finite element model was used to simulate the EMR device as this approach has been demonstrated in literature to correspond well with experimental data on InSb/metal EMR devices.[1, 24] All simulations were performed using COMSOL Multiphysics software.

For the case of a thin film device, electronic motion in the z-direction can be ignored as the electrons are constrained to a plane. In such a two-dimensional system with a purely diffusive transport mode, the constitutive equation between the current density, $\mathbf{j}$, and electric field, $\mathbf{E}$, in the presence of a magnetic field, $\mathbf{B}$, oriented perpendicular to the plane of the device takes the form of:

$$j_i = \sigma_{ij}(B)E_j \tag{4}$$

where σ is the magnetoconductivity tensor given by:

$$\sigma(\mathbf{B}) = \frac{\sigma_0}{1+\beta^2}\begin{bmatrix} 1 & -\beta \\ \beta & 1 \end{bmatrix} \tag{5}$$

Here,

$$\sigma_0 = ne\mu \quad ; \quad \beta = \mu B$$

where σ_0 is the conductivity in the absence of a magnetic field, n is the carrier density, μ is the carrier mobility, and e is the fundamental charge.[1]

We model the behavior of the device when subjected to a uniform magnetic field in the range from -1 T to 1 T, as the model has been fully validated under these conditions by comparison with experimental results.[1] The properties of InSb were used to model the semiconductor material whereas those of Au were chosen for the metal. Carrier mobilities of 45,500 $\mathrm{cm^2V^{-1}s^{-1}}$ and 53 $\mathrm{cm^2V^{-1}s^{-1}}$ and carrier densities of $2.55 \cdot 10^{16}$ $\mathrm{cm^{-3}}$ and $5.90 \cdot 10^{22}$ $\mathrm{cm^{-3}}$ were used for the semiconductor and metal portions, respectively.[25]

1.2. Device Geometry

Defining the angle to be $\theta = 0°$ when the slot is in the N-position in Fig. 1, we consider a device geometry where the two voltage probes are located at 45° and 315°, the current lead at 135°, and the ground lead at 225°. Each contact spans an angular width of 10°. Regarding the location of a slot, as also shown in Fig. 1, we denote the angular position of 0° as North (N), 90° as West (W), 180° as South (S) and 270° as East (E), respectively.

The absolute size of the device does not influence the computed values of the four-terminal resistance, magnetoresistance, or sensitivity, with the exception that the resisitance and sensitivity are inversely proportional with the thickness of the device. In this work a thickness of 1.3 μm is used.

To ensure numerical convergence of the model, in Fig. 2 we show the resistance and magnetoresistance at 1 T of the modeled device both for the concentric device with no slot and for the case of a single slot placed at the North position as a function of the number of mesh elements in the finite element model. We consider a slot with a depth of $0.7(r_o - r_i)$, i.e. extending 70% into the semiconductor disc, and angular span of $\phi = 10°$. It can be seen that decreasing the number of mesh elements increases MR and R below a certain threshold. This is due to fact that path of the carriers is longer as a result of the larger mesh elements. All of the models presented herein have more than 10000 mesh elements to ensure convergence of the numerical results.

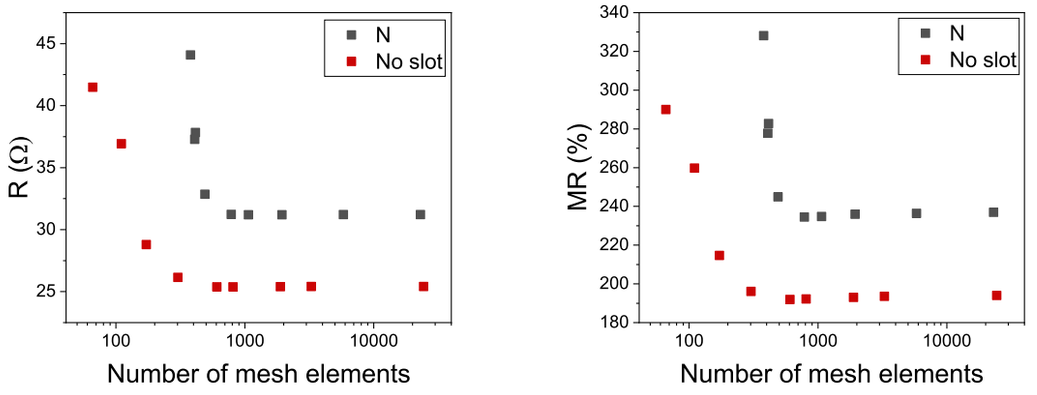

Figure 2: Resistance (left) and magnetoresistance (right) at 1 T of devices with and without a slot in the N position as a function of the number of mesh elements.

2. Results and Discussion

2.1. Circular Sensor

We begin by investigating the influence of a slot on the performance of a concentric EMR device, specifically the effect of the size and placement of a slot. The slot has an angular span of $\phi = 10°$ unless otherwise stated.

2.1.1. Single Slot with Fixed Position

We first consider the effect of adding a single outer slot to the semiconductor disc. In Fig. 3 we show the current flow for the case when a single slot is located in the north position, i.e. $\theta = 0°$, for two different magnetic flux densities. When $B = 0$ T nearly all of the current flows through the inner metal disc and bypasses the upper region of the semiconductor altogether, regardless of the presence or absence of a slot. However, when $B = 1$ T a portion of the current is expelled from the gold and forced around the outer boundary. Here the slotted geometry increases the resistance of the device even further by reducing the cross-sectional area that the current can pass through.

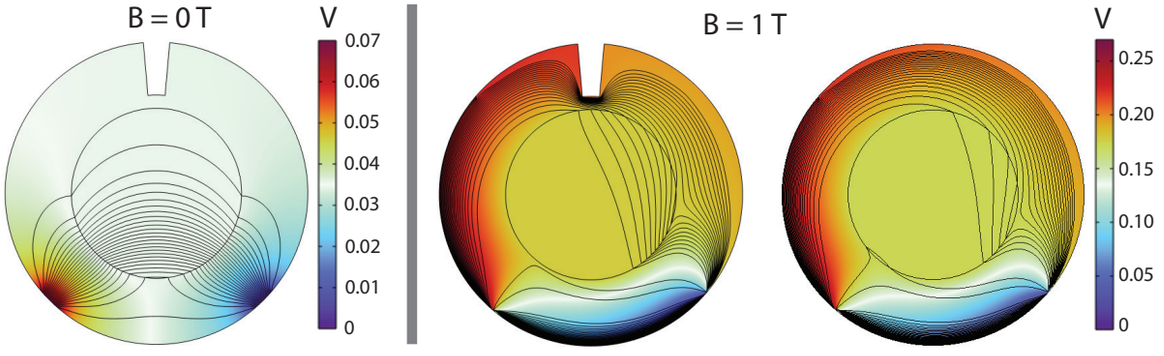

Figure 3: Current flow (black lines) and voltage in $B = 0$ T (left) and $B = -1$ T (right) for the slotted geometry. Shown on the right is also a standard concentric device for comparison at $B = 1$ T. The case of $B = 0$ T for the standard concentric device is not shown for brevity, as it is identical to the slotted case.

In Fig. 4a and b the magnetoresistance and sensitivity at 1 T are shown as functions of the ratio of the radii of the semiconductor and metal discs, traditionally termed α, and the slot depth, d_s, for

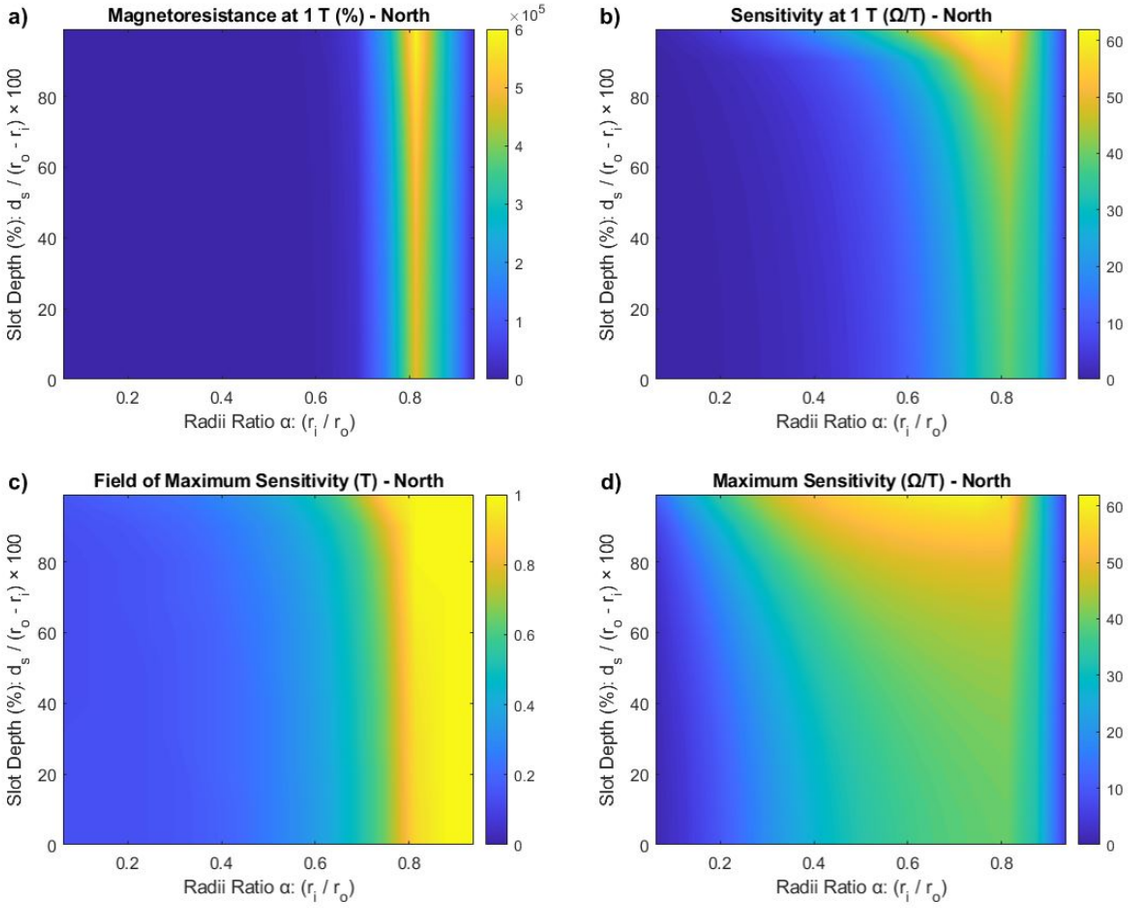

Figure 4: (a) Magnetoresistance and (b) sensitivity at 1 T for a sensor with a slot in the N position for varying slot depths and ratios of the inner to outer radii. Also shown are (c) the field at which the maximum sensitivity occurs for a given geometry and (d) the magnitude of the maximum sensitivity.

a slot at the N position. The magnetoresistance is strongly dependent on the value of α with a sharp peak around a value of 13/16, as has been observed in previous literature.[1, 4, 21, 18] The presence of a slot does increase the measured magnetoresistance, however the effect of slot depth is relatively weak by comparison. Only a 20% improvement over the standard geometry is seen in the case of the highest slot depth at 1 T and the difference is negligible at weak fields. The high-field resistance of the device is higher for the slotted case, but an relative increase in the zero-field resistance tempers the subsequent gain in magnetoresistance. Considering that modifications to the shape of the metallic shunt can increase the magnetoresistance by several orders of magnitude[17, 18, 19], modifying the perimeter with a slot in the north position does not appear to be an effective way to boost this parameter. The sensitivity on the other hand is typically more difficult to increase but can be significantly impacted by placing a slot. A deep slot can increase the maximum sensitivity by 70% relative to the best performing unslotted device as can be seen in Fig. 4d. The improvement in the sensitivity is a direct consequence of the higher overall resistance in the sensor. It is also interesting to examine how d_s and α influence the sensitivity. For d_s the relationship seems straightforward; a deeper slot always yields a higher sensitivity. But in the case of α, while the range of values which produce a high sensitivity at a given slot depth is broad, the field at which the maximum sensitivity is reached can vary dramatically, as shown in Fig. 4c. This suggests that by changing the ratio of the radii the sensor can be tuned to operate best around

the field range that is of most interest to the user. As can be seen in the bottom sub-figures, a high sensitivity can be obtained even at relatively low magnetic fields if high slot depths and low α values are used. A high sensitivity is more critical than magnetoresistance for obtaining sensors with a good field resolution and is also more difficult to obtain, thus making these findings particularly interesting for sensor design.[26]

2.1.2. Rotating a Slot

Having demonstrated that a slot can have a positive effect on the high-field magnetoresistance as well as the sensitivity generally, we now consider the effect of rotating a single outer slot around the circumference of the EMR device. The slot cannot be placed in the angular sections spanned by the contacts, so these areas are excluded in the study. We begin by placing the slot in the N position ($\theta = 0°$) and rotating it counterclockwise. The slot has a depth of 90% and angular span of $\phi = 10°$ and we consider a device with $\alpha = 10/16$.

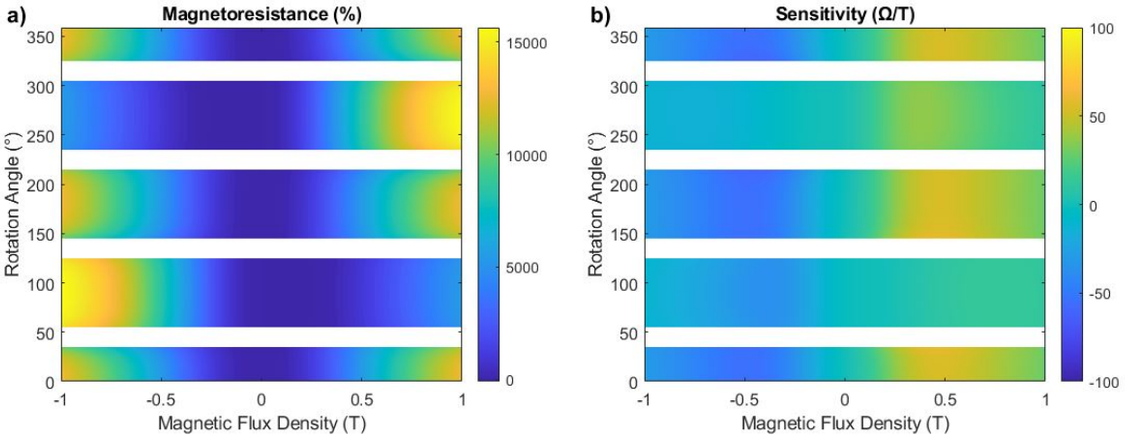

Figure 5: (a) Magnetoresistance and (b) sensitivity as functions of the magnetic field and rotational angle of the slot for a device with $\phi = 10°$, $d_s = 0.9(r_o - r_i)$, and $\alpha = 10/16$.

In Fig. 5 it can be observed that when the slot is in the N and S positions the symmetry of the device is preserved and the resistances in both of these cases are identical and symmetric about 0 T. For the E and W cases, the mirror symmetry is broken which causes the response to be asymmetric about 0 T and mirror symmetric to each other. The exact value of the rotational angle has little effect, it is which pair of contacts the slot is placed between that determines the overall behavior. Since the N/S cases are identical, the E/W cases are mirror symmetric, and as all other angles yield results similar to these points we will only discuss the results of moving the slot from the N position to the W position. The resistance curves as a function of magnetic field of slotted and unslotted devices with different values of α are shown in Fig. 6a and b.

For the case of the W slot, the resistance of the device when the field is positive is relatively invariant but is similar to that of the unslotted device when the field is oriented in the negative direction. As a result, at positive fields the magnetoresistance is negligible but at negative fields it reaches values up to 80% higher than the unslotted geometry, primarily due to a lower zero-field resistance. Fig. 6c and d also show the sensitivity of devices with various values of α for the unslotted and W slotted cases. The magnitude of the maximum sensitivity and location the peak is similar for both sets of geometry. For the unslotted geometry the sensitivity is always 0 Ω/T at 0 T, but the introduction of a slot in the W position results in finite zero-field values of the sensitivity.

Measurements of weak magnetic phenomena require sensors with a high zero-field sensitivity. Achieving this without the introduction of a bias field to move the performance of the sensor into a field range where it is sensitive greatly simplifies sensor fabrication and calibration. Other works have shown that

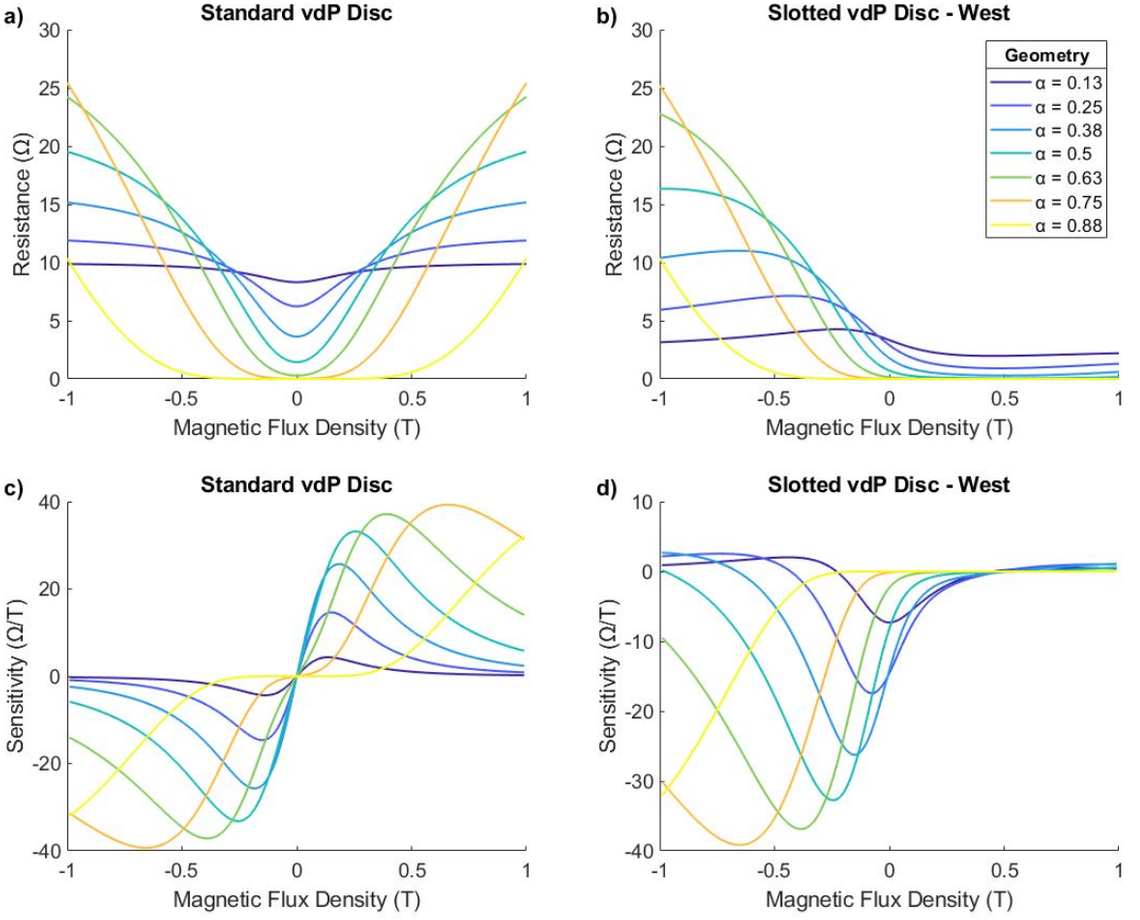

Figure 6: Resistance as a function of magnetic field for various values of α in the standard unslotted geometry (a) and device with a slot in the W position (b). Sensitivity as a function of magnetic field for various values of α in the standard (c) and slotted (d) geometries.

the zero-field sensitivity can be increased by breaking the symmetry of the device, either by shifting the location of the shunt or the contacts such that the symmetry is broken.[24, 27, 28] We show that the introduction of a slot between the voltage and current contacts also breaks this symmetry and allows for a finite zero-field sensitivity. In Fig. 7a we show that for a slot in the W position, there are a range of geometries where the maximum sensitivity is obtained at $B = 0$ T. The corresponding maximum sensitivity for each geometry is shown in Fig. 7b. In Fig. 7c we show the magnitude of the sensitivity at 0 T for all slot positions, i.e. as function of the slot rotation angle. As can be seen from the figure, the zero-field sensitivity is maximized at the E and W positions. As long as the slot is located between opposite pairs of contacts, the zero-field sensitivity is relatively invariant as a function of the rotational angle. However, when placed between like contacts, the rotational angle has a large effect, with rapid increases in the zero-field sensitivity as the slot is moved further away from the vertical positions. In Fig. 7d we also examine the effect that α and d_s have for a slot in the W position and determine that the optimal geometry for achieving a high zero-field sensitivity is one with as large a slot depth as possible and $\alpha \approx 0.3$.

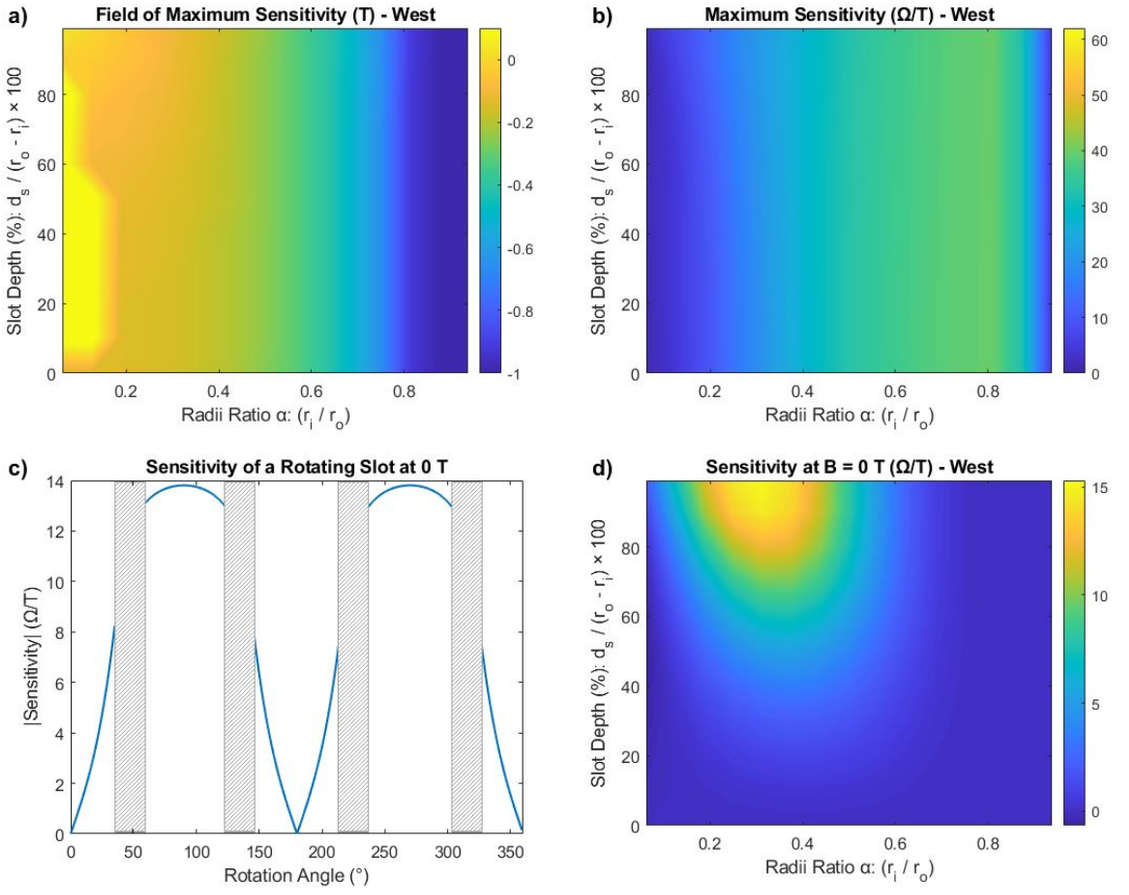

Figure 7: (a) The field at which the maximum sensitivity occurs for the W slot case and (b) the magnitude of the maximum sensitivity. (c) Absolute value of the sensitivity at zero-field as a function of the rotational angle of the slot for $\alpha = 6/16$ and (d) as functions of α and d_s for a slot in the W position.

2.1.3. Inner vs Outer Slot

Until now, we have only considered a slot placed at the outer circumference of the device. However, as shown in Fig. 1 the slot can also be placed on the inner circumference of the semiconductor disc. To compare these two cases, we have computed the resistance as function of magnetic field for both inner and outer slots placed at the north and west positions. In both cases we find that whether the slot originates at the inner or outer circumference the performance of the device display almost exactly the same trends as discussed above, suggesting that it is the angular position and size of the constriction which are most important rather than its exact boundary placement.

2.1.4. Slot Depth and Angular Span

The cases discussed thus far have explored variations in the depth and position of the slot. However, it is clearly of interest to investigate the effect of the width of the slot, as defined by its angular span. Therefore, we have modeled a single outer slot placed at either the north or west positions, with a varying angular span ϕ and slot depth d_s.

Shown in Fig. 8 are the magnetoresistance and sensitivity for N and W slots as a function of both the slot depth and angular span for a magnetic field of 1 T for a fixed $\alpha = 10/16$. As can be seen in Fig. 8a, for the case of the N slot the magnetoresistance increases monotonically with slot depth for all

widths. The optimal N slot geometry for achieving a high field magnetoresistance is a deep slot with an angular span of around 40°, although the range of angular spans which can be used is wide. For a high sensitivity, deeper and wider slots produce better results. In the case of the W slot, the results are more nuanced. When the field is oriented in the positive direction, there is a negative correlation between the slot depth and slot width which yield the highest magnetoresistances. There is a band of possible slot depths that are optimal for a given slot width, though the depths spanned by this band tend to become shallower as the slot width is increased. When the field is oriented in the negative direction however, the high-field magnetoresistance is large and mostly invariant as a function of depth and width, provided the slot is deeper than roughly 40%.

It should also be noted that the field at which the maximum sensitivity occurs is very weakly dependent on slot depth in the N slot case and completely independent in the W slot case as can be seen in Fig. 8. This indicates that the location of the maximum sensitivity depends almost entirely on the value of α and not the size, shape, or even presence of a slot. The maximum sensitivity for the W slot is lower than that of the N slot and approximately the same as that of the unslotted geometry. It can therefore be concluded that adding a constriction along the N/S axis of the device is beneficial for increasing the maximum sensitivity, whereas placing the constriction across the E/W axis does not increase the maximum sensitivity but does open up a finite sensitivity at low fields. However, the conclusion remains that for sensitivity at a given field, a slot will be highly beneficial.

2.2. Elliptical Sensor

Having shown how deforming the outer boundary of an EMR device by using slots can affect the magnetoresistance and sensitivity, we now examine the effect of a more continuous type of deformation by removing the constraint that the sensor is circular and increasing the ellipticity of the outer boundary.

We consider a device where the metal component has a circular geometry with a radius r_i. Rather than being defined by a single radial parameter, r_o, the outer boundary is now instead defined by the lengths of semi-major and semi-minor axes, a and b. Two scenarios are presented: the first, where the length of the semiaxes a/r_i and b/r_i are varied from 1.05 to 2, and the second, where the angular position of the contacts is held constant but the ellipse is rotated. Again, we note the absolute size of the device does not impact the resistance, magnetoresistance or sensitivity of the device, as the thickness of the device is kept constant. As such we present all device dimensions in terms of their relative ratios. A schematic of the elliptical sensor can be seen in Figure 9.

2.2.1. Effect of Varying Semiaxis Length

Varying the a and b semiaxes without rotating the ellipse ($\theta = 0$) yields different results as shown in Fig. 10, demonstrating that narrowing or extending the semiconductor layer in the N-S or E-W directions has a significant effect on device performance. The high-field magnetoresistance shows a strong peak as a function of the length of the b-semiaxis. This peak occurs around a value $b/r_i = 1.25$, which would correspond to an α of 13/16 in the circular geometry where it also produces the largest high-field magnetoresistance. This suggests that the geometric parameter that controls magnetoresistance is the width of the semiconductor in the region between the voltage probes. Modifying the length of the a-semiaxis produces a smaller but still significant effect. A longer horizontal semiaxis reduces magnetoresistance, while shorter lengths increase it; a direct result of the effect of the horizontal width on the zero-field resistance of the sensor. The shorter the distance between the source and drain contacts and the shunt, the smaller the zero-field resistance, and the higher the measured magnetoresistance. The highest magnetoresistances observed within the range of semiaxis length variations tested was 30% higher than for a standard vdP geometry and similar to the highest values attained in the case of the device with a slot in the N position.

With regards to the sensitivity, high values are only reached when the horizontal semiaxis is short and the vertical semiaxis is much longer, i.e. a horizontal semiaxis $\alpha \geq 14/16$ and eccentricity $e \geq 0.6$. The maximum sensitivity saturates around this point, reaching a value of 120 Ω/T, twice as high as the largest value observed in the slotted cases. Thus it can be said that with regards to the maximum sensitivity, increasing the resistance between the probes and the conductive inclusion

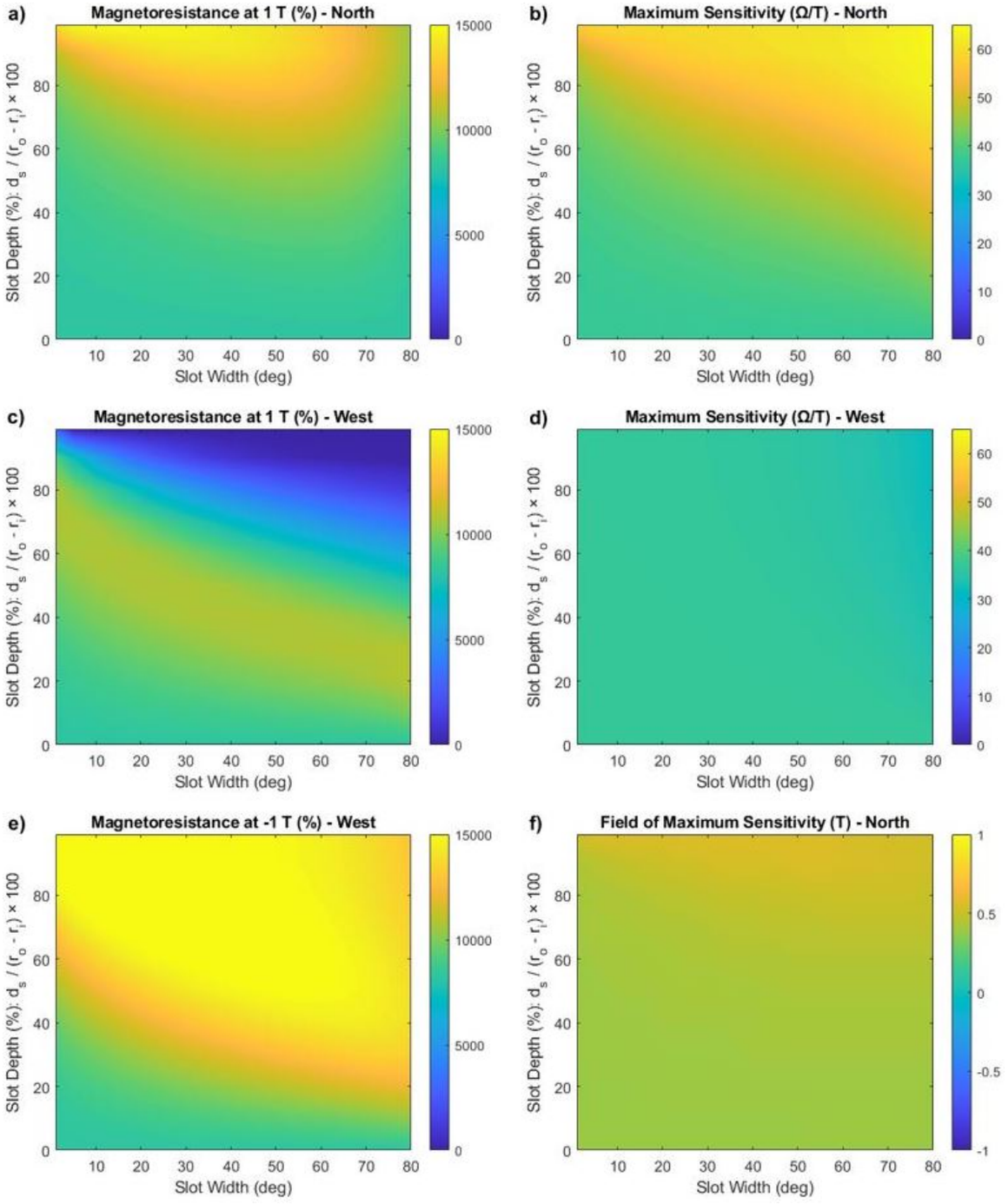

Figure 8: Magnetoresistance at 1 T as a function of slot depth, d_s, and width, ϕ, for a slot in the (a) N and (c) W positions. (e) Also shown is the magnetoresistance at -1 T for a slot in the W position. Maximum sensitivity as a function of slot size for the (b) N and (d) W positions. (f) Field strength which yields a maximum sensitivity for a slot in the N position.

is beneficial. However the highest sensitivities for these geometries were found at high fields, above

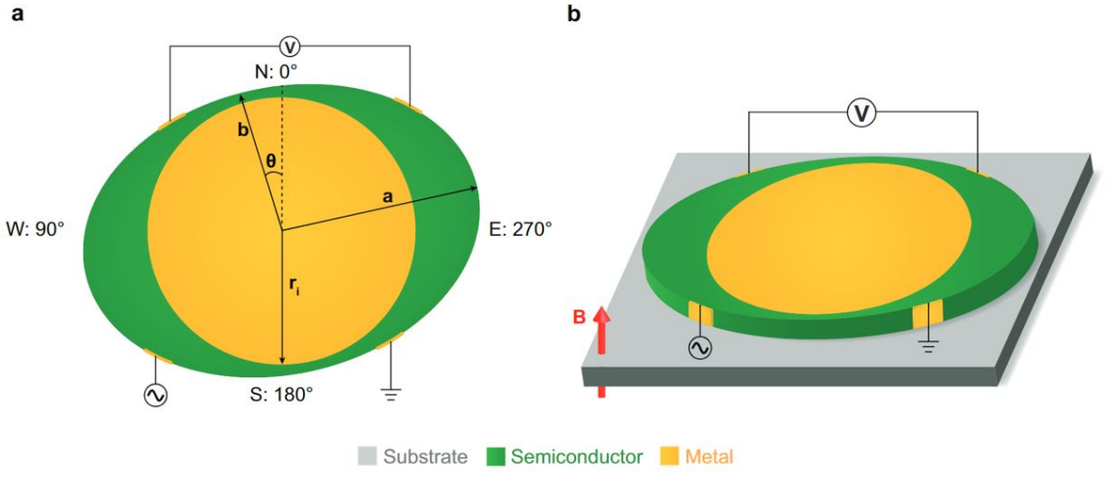

Figure 9: Conceptual figure of an elliptical sensor. (a) The various parameters which we use to define the geometry of the sensor and of the deformations to the boundary. (b) A 3D view of the sensor in operation under an applied magnetic field.

0.6 T. Regardless, it can be concluded that relaxing the requirement of circular geometries offers the possibility of significantly improving the high-field sensitivity of EMR devices.

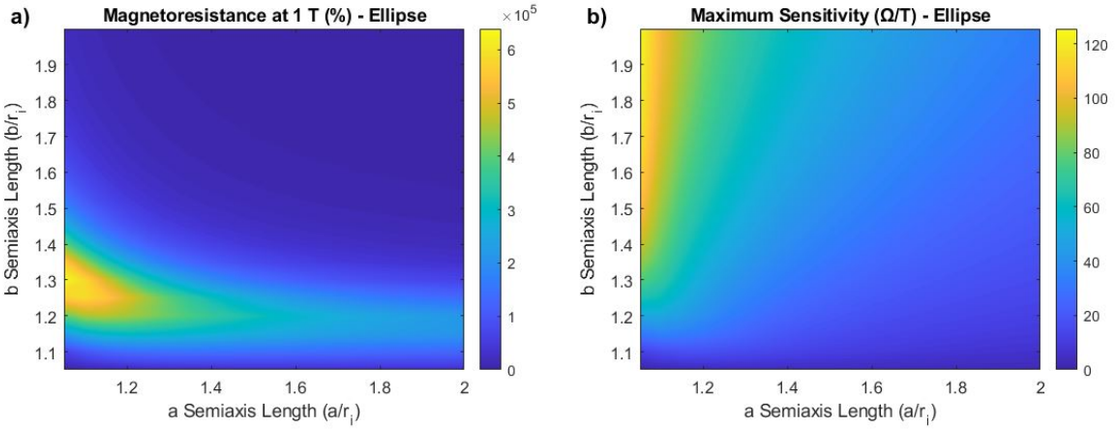

Figure 10: (a) Magnetoresistance at 1 T and (b) maximum sensitivity for an elliptical sensor with varying lengths of the major and minor semiaxes.

2.2.2. Rotating Ellipse

We also present the case of an ellipse with a fixed a/b ratio where the semi-major and semi-minor axes are rotated by an angle, θ, as shown in Figure 9. The angular position and angular span of the contacts were held fixed as the boundary of the sensor was rotated. For this study we evaluate two geometries based on the results of the previous simulations: the ellipses that yielded the highest magnetoresistance ($a/r_i = 1.05$, $b/r_i = 1.3$, $e = 0.59$) and sensitivity ($a/r_i = 1.05$, $b/r_i = 2.0$, $e = 0.85$), respectively.

A strong angular dependence was observed for the high field magnetoresistance. Vertically orienting an ellipse with $e = 0.59$ resulted in an increase in the magnetoresistance by a factor of 3 when compared to a horizontal orientation. However, for ellipses with a higher eccentricity the highest magnetoresistances were found when the long semiaxis of the sensor was rotated $\pm 45°$ from horizontal and were one order of magnitude greater than their horizontal orientation. This peak in rotational angle is quite sharp and the effect quickly drops off as the ellipse is rotated. On the other hand, examining the sensitivity as a function of rotational angle shows that the greatest sensitivities are obtained when the long semiaxis is more or less aligned horizontally. The sensitivity is much more insensitive to the precise value of the rotational angle, as values close to the peak are still reached when $\theta = 0 \pm 20°$.

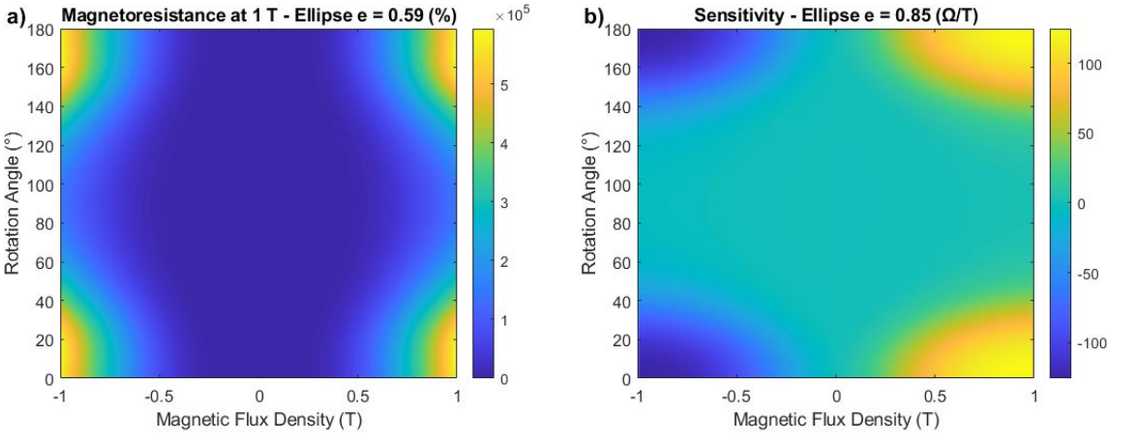

Figure 11: (a) Magnetoresistance and (b) sensitivity of an elliptical sensors as a function of the rotational angle and magnetic field.

2.3. Detection Limit and Noise-Equivalent Field

Of particular importance when designing magnetic sensors is the detection limit. This value is commonly referred to as the noise-equivalent field, B_{NEF}, and is defined as the strength of the magnetic field which produces a signal as large as the noise. If the sensor is driven with low frequencies of alternating current the noise generally scales with frequency as $1/f$, whereas at high frequencies the noise is primarily dominated by thermal fluctuations and is frequency independent. In the thermal-noise regime, B_{NEF} is given by the following equation:

$$B_{NEF}^{thermal} = \frac{\sqrt{4k_B T R_{V,2pt}(B_{bias})}}{I\left|\frac{dR}{dB}\right|_{B_{bias}}} \tag{6}$$

where k_B is the Boltzmann constant, T is the temperature, $R_{V,2pt}(B_{bias})$ is the two-point resistance between the voltage probes at a given bias magnetic field, and I is the current supplied to the device [8]. For our analysis, we assume a current of 130 µA and room temperature operation, as based on literature values of high mobility InSb thin films of a similar thickness [8].

In Figure 12 we show a comparison of some of the geometries discussed in this work in terms of their minimum B_{NEF}. For reference, a standard vdP disc with $\alpha = 12/16$ (Fig.12a) has a minimum $B_{NEF} = 36$ nT/$\sqrt{\text{Hz}}$ at a bias field of 0.66 T. This value is comparable with experimental results in literature.[8] Adding a slot $d_s = 0.99$ in the N position (Fig.12b) lowers the minimum B_{NEF} by 21% to 28.3 nT/$\sqrt{\text{Hz}}$, but shifts the bias field to a higher value of 0.93 T. The same slot configuration for a lower α of 5/16 (Fig.12c) leads to a reduction in B_{NEF} by 32% to 24.5 nT/$\sqrt{\text{Hz}}$ and also shifts the required bias field to a much lower value of 0.24 T. Rotating the position of the slot to the W position

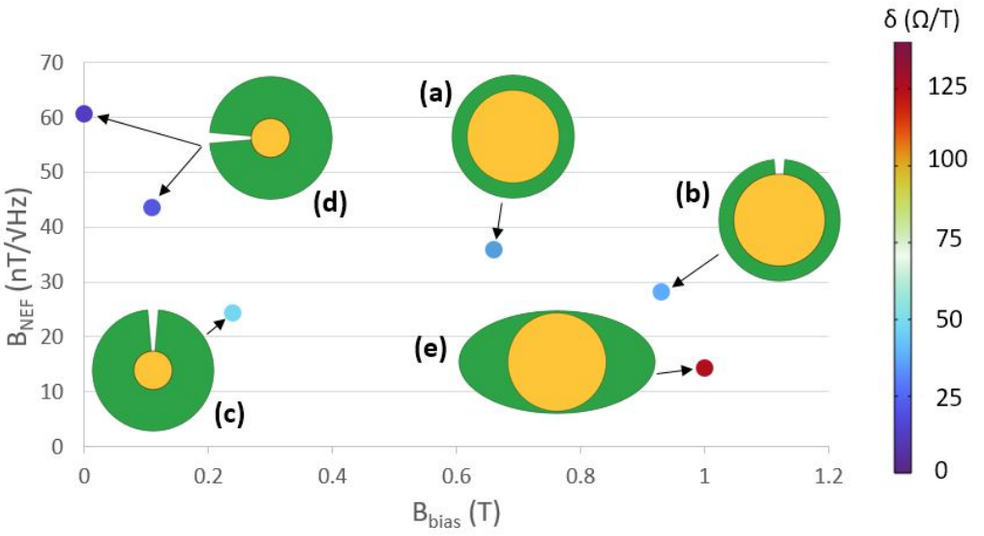

Figure 12: Minimum field resolution, B_{NEF}, at the field, B_{bias}, which yields the highest sensitivity, δ, for selected geometries: a) Standard vdP disc with $\alpha = 12/16$; b) N slot, $d_s = 0.99$, $\alpha = 12/16$; c) N slot, $d_s = 0.99$, $\alpha = 5/16$; W slot, $d_s = 0.99$, $\alpha = 5/16$; and ellipse, $\theta = 0°$, $a/r_i = 1.05$, $b/r_i = 2$. The color of each data point represents the absolute value of the sensitivity at B_{bias}.

(Fig.12d) increases the minimum B_{NEF} by 22% to 43.6 nT/$\sqrt{\text{Hz}}$ and shifts the bias field to a very low value of 0.11 T. Though the maximum sensitivity is nearly half that of the standard sensor, a lower $R_{V,2pt}$ is able to partially compensate in order to produce reasonably good B_{NEF}. Additionally this particular configuration yields a finite field resolution with zero bias field, although at to 60.6 nT/$\sqrt{\text{Hz}}$ it is 38% higher than the minimum value for this geometry and 70% higher than the minimum value for the standard geometry. Finally, an elliptical configuration with a low a/b ratio (Fig. 12e) produced the lowest B_{NEF} of all designs evaluated in this study. The minimum B_{NEF} of the elliptical sensor was found to be to 14.3 nT/$\sqrt{\text{Hz}}$, 70% lower than the standard geometry, although a high bias field of 1 T is required to reach this value. This low value is a result of the much higher sensitivity but is partly tempered by a large $R_{V,2pt}$.

3. Conclusion

The work has shown how two discrete types of changes to the geometry of the semiconductor portion of an EMR sensor can modify its performance. The presence and size of a slot can moderately boost the magnetoresistance or significantly increase the sensitivity when compared to an unmodified sensor, depending on where it is in relation to the contacts. Slots placed between a pair of similar contacts were found to increase the maximum sensitivity, whereas a respectable zero-field sensitivity was observed when placed between opposite pairs of contacts which could be of interest for applications where the sensing of weak magnetic fields is required. Changes in the location of the shunt have been shown to produce four times higher zero-field sensitivities [24] than the results presented herein, however it is still of interest to note that the shape of the boundary can also play a significant effect. With regards to the sensitivity, we also find that the optimal value of α depends on the desired measurement field, with smaller ratios of around 0.375 being preferable for low fields. A continuous deformation of the sensor boundary into an ellipse was also shown to increase the high field sensitivity of the sensors when the major semiaxis was oriented vertically. Rotating the major semiaxis of this ellipse by $\pm 45°$ was shown to be beneficial for improving the high-field magnetoresistance if that is the figure of merit that

is of interest. Based on the results of this study we can conclude that magnetoresistance is primarily driven by the value of α, in particular the thickness of the semiconductor regions between like pairs of probes and the shunt. Maximum sensitivity can be increased by increasing the resistance of the region of material between like pairs of probes whereas a zero-field sensitivity can be induced by breaking the vertical symmetry of the device. These results indicate that the geometry of the semiconductor represents an additional degree of freedom for tuning the response of the sensor.

With regards to the detection limit, based on our results we can conclude that large slot depths in either the N or W positions and α values of 5/16 or slightly larger are preferable for designing sensors with a low bias field and a good minimum field resolution. A slot in the N position has a lower B_{NEF} but requires a higher bias field while a slot in the W position has a worse B_{NEF} but requires little to no bias field to operate. Elliptical sensors produce the best B_{NEF} values in our study but the high bias field required makes them more practical for performing high-field measurements.

It is unlikely that the geometries presented herein represent the optimum points in this parameter space, but rather serve as examples to elucidate the principle of shape optimization. Future studies may benefit from examining the effects of multiple slots or more complex deformations of the sensor boundary in order to investigate whether higher magnetoresistances or sensitivities can be achieved via this principle.

4. Acknowledgements

The authors acknowledges the support of Novo Nordisk Foundation Challenge Programme 2021: Smart Nanomaterials for Applications in Life-Science, BIOMAG Grant NNF21OC0066526. D.V.C. also acknowledges the support of Novo Nordisk Foundation NERD Programme: New Exploratory Research and Discovery, Superior Grant NNF21OC0068015.

References

[1] J. Moussa, L. R. Ram-Mohan, J. Sullivan, T. Zhou, D. R. Hines, and S. Solin. Finite-element modeling of extraordinary magnetoresistance in thin film semiconductors with metallic inclusions. *Physical Review B*, 64, 2001.

[2] S. Di Ventra, M. Evoy and J. R. Heflin, editors. *Introduction to Nanoscale Science and Technology*, chapter Magnetoresistive Devices and Materials. Springer, Boston, USA, 2004.

[3] L. A. Francis and K. Poletkin, editors. *Magnetic Sensors and Devices: Technologies and Applications*, chapter Giant (GMR) and Tunnel (TMR) Magnetoresistance Sensors: From Phenomena to Applications, pages 35–65. CRC Press, 2017.

[4] S. Solin, T. Thio, D. R. Hines, and JJ. Heremans. Enhanced room-temperature geometric magnetoresistance in inhomogeneous narrow-gap semiconductors. *Science*, 289:1530–1532, 2000.

[5] D. Kleinman and A. Schawlow. Corbino disk. *Journal of Applied Physics*, 31(12), 1960.

[6] M. Kamada, V. Gall, J. Sarkar, M. Kumar, A. Laitinen, I. Gornyi, and P. Hakonen. Strong magnetoresistance in a graphene corbino disk at low magnetic fields. *Physical Review B*, 104, 2021.

[7] C.H. Möller, O. Kronenwerth, D. Grundler, W. Hansen, C. Heyn, and D. Heitmann. Extraordinary magnetoresistance effect in a microstructured metal-semiconductor hybrid structure. *Applied Physics Letters*, 20, 2002.

[8] S.N. Sahu, R. K. Choudhury, and P. Jena, editors. *Nano-Scale Materials: From Science to Technology*, chapter Design and Properties of a Scanning EMR Probe Microscope. Nova Science Publishers, 2006.

[9] A. S. Troup, D. G. Hasko, J. Wunderlich, and D. A. Williams. Magnetoresistance in silicon-based semiconductor-metal hybrid structures. *Applied Physics Letters*, 89, 2006.

[10] S. Pisana, P. M. Braganca, E. E. Marinero, and B. A. Gurney. Tunable nanoscale graphene magnetometers. *Nano Letters*, 10, 2010.

[11] J. Lu, H. Zhang, W. Shi, Z. Wang, Y. Zheng, T. Zhang, N. Wang, Z. Tang, and P. Sheng. Graphene magnetoresistance device in van der pauw geometry. *Nano Letters*, 11(7), 2011.

[12] D. C. Wu, Y. W. Pan, J. S. Wu, S. W. Lin, and S. D. Lin. High-sensitivity two-terminal magnetoresistance devices using InGaAs/AlGaAs two-dimensional channel on GaAs substrate. *Applied Physics Letters*, 108, 2016.

[13] S. El-Ahmar, W. Koczorowski, A. A. Poźniak, P. Kuświk, M. Przychodnia, and J. Dembowiak W. Strupiński. Planar configuration of extraordinary magnetoresistance for 2d-material-based magnetic field sensors. *Sensors and Actuators, A: Physical*, 296:249–253, 2019.

[14] L.Wang, I. Meric, P.Y. Huang, Q. Gao, Y. Gao, H. Tran, T. Taniguchi, K. Wantabe, L. M. Campos, D. A. Muller, G. Juo, P. Kim, J. Hone, K. L. Shepard, and C. R. Dean. One-dimensional electrical contact to a two-dimensional material. *Science*, 342:614–617, 2013.

[15] C. R. Dean, A. F. Young, I. Meric, C. Lee, L. Wang, S. Sorgenfrei, K. Watanabe, T. Taniguchi, P. Kim, K. L. Shepard, and J. Hone. Boron nitride substrates for high-quality graphene electronics. *Nature Nanotechnology*, 5:722–726, 2010.

[16] B. Zhou, K. Watanabe, T. Taniguchi, and E. A. Henriksen. Extraordinary magnetoresistance in encapsulated monolayer graphene devices. *Applied Physics Letters*, 216, 2020.

[17] T. Huang, L. Ye, K. Song, and F. Deng. Planar structure optimization of extraordinary magnetoresistance in semiconductor–metal hybrids. *Journal of Superconductivity and Novel Magnetism*, 27:2059–2066, 2014.

[18] T. Hewett and F. V. Kusmartsev. Geometrically enhanced extraordinary magnetoresistance in semiconductor-metal hybrids. *Physical Review B - Condensed Matter and Materials Physics*, 82 (21), 2010.

[19] Z. Moktadir and H. Mizuta. Magnetoresistance in inhomogeneous graphene/metal hybrids. *Journal of Applied Physics*, 113(8), 2013.

[20] R. Erlandsen. *Enhancing the extraordinary magnetoresistance by variations in geometry and material properties*. PhD thesis, Technical University of Denmark, 2022.

[21] T. Zhou, S. Solin, and D. R. Hines. Extraordinary magnetoresistance of a semiconductor-metal composite van der pauw disk. *Journal of Magnetism and Magnetic Materials*, page 226–230, 2001.

[22] J. Sun and J. Kosel. Finite element analysis on the influence of contact resistivity in an extraordinary magnetoresistance magnetic field micro sensor. *Journal of Superconductivity and Novel Magnetism*, 25(8):2749–2752, 2012.

[23] T. Zhou, D. R. Hines, and S. Solin. Extraordinary magnetoresistance in externally shunted van der pauw plates. *Applied Physics Letters*, 78(5):667–669, 2001.

[24] R. Erlandsen, R. Bjørk, L. Kornblum, N. Pryds, and D. V. Christensen. Symmetry breaking in magnetoresistive devices. *Physical Review B*, 106(1), 2022.

[25] J. Sun and J. Kosel. Finite-element modelling and analysis of hall effect and extraordinary magnetoresistance effect. *Finite Element Analysis - New Trends and Developments*, 2012.

[26] T. Désiré Pomar, R. Erlandsen, B. Zhou, L. Iliushyn, R. Bjørk, and D. V. Christensen. Extraordinary magnetometry - a review on extraordinary magnetoresistance. *arXiv*, 2022.

[27] S. Solin and T. Zhou. Extraordinary magnetoresistance of an off-center van der pauw disk. *Extended Abstracts of the 2001 International Conference on Solid State Devices and Materials*, 1, 2001.

[28] M. Holz, O. Kronenwerth, and D. Grundler. Enhanced sensitivity due to current redistribution in the hall effect of semiconductor-metal hybrid structures. *Applied Physics Letters*, 86(7), 2005.

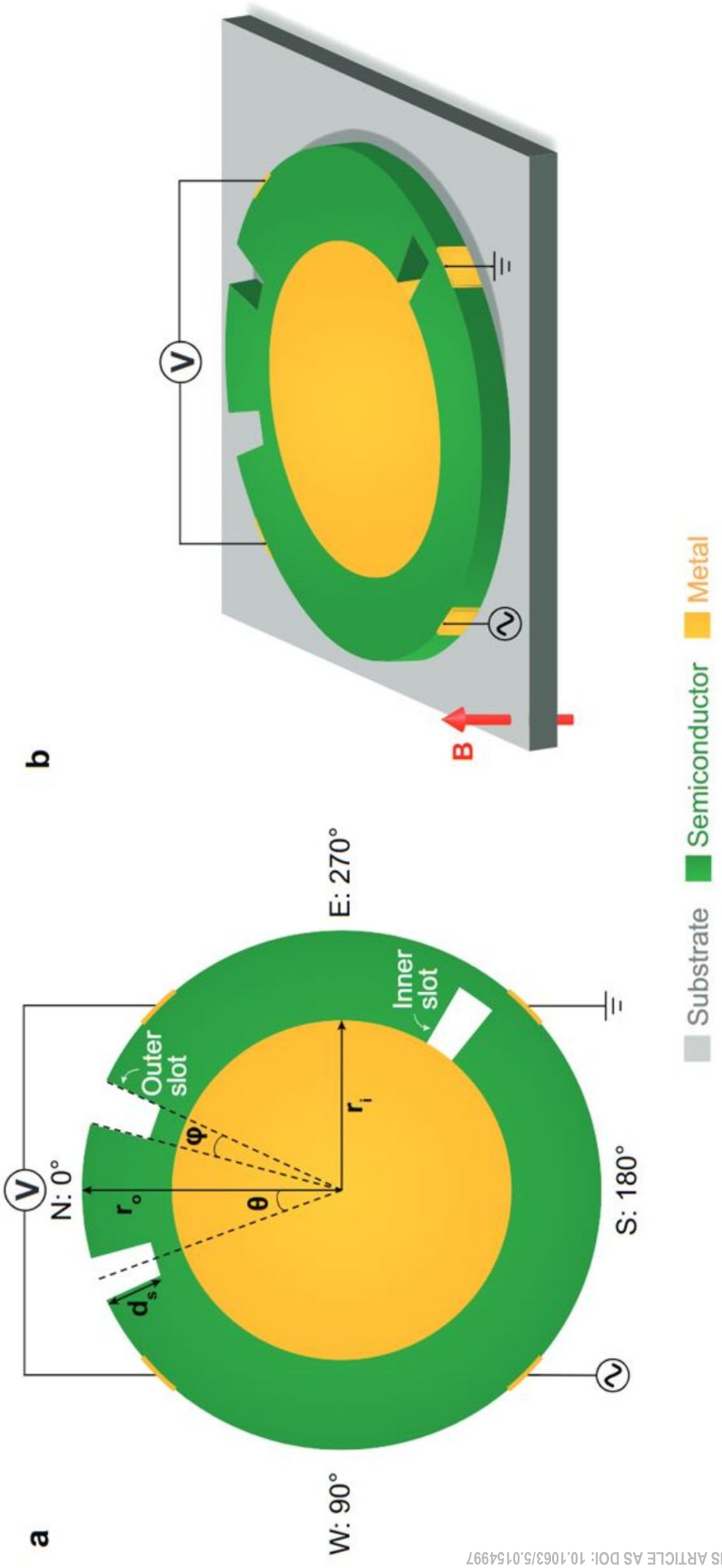

AIP Publishing

Journal of Applied Physics

ACCEPTED MANUSCRIPT

This is the author's peer reviewed, accepted manuscript. However, the online version of record will be different from this version once it has been copyedited and typeset.
PLEASE CITE THIS ARTICLE AS DOI: 10.1063/5.0154997

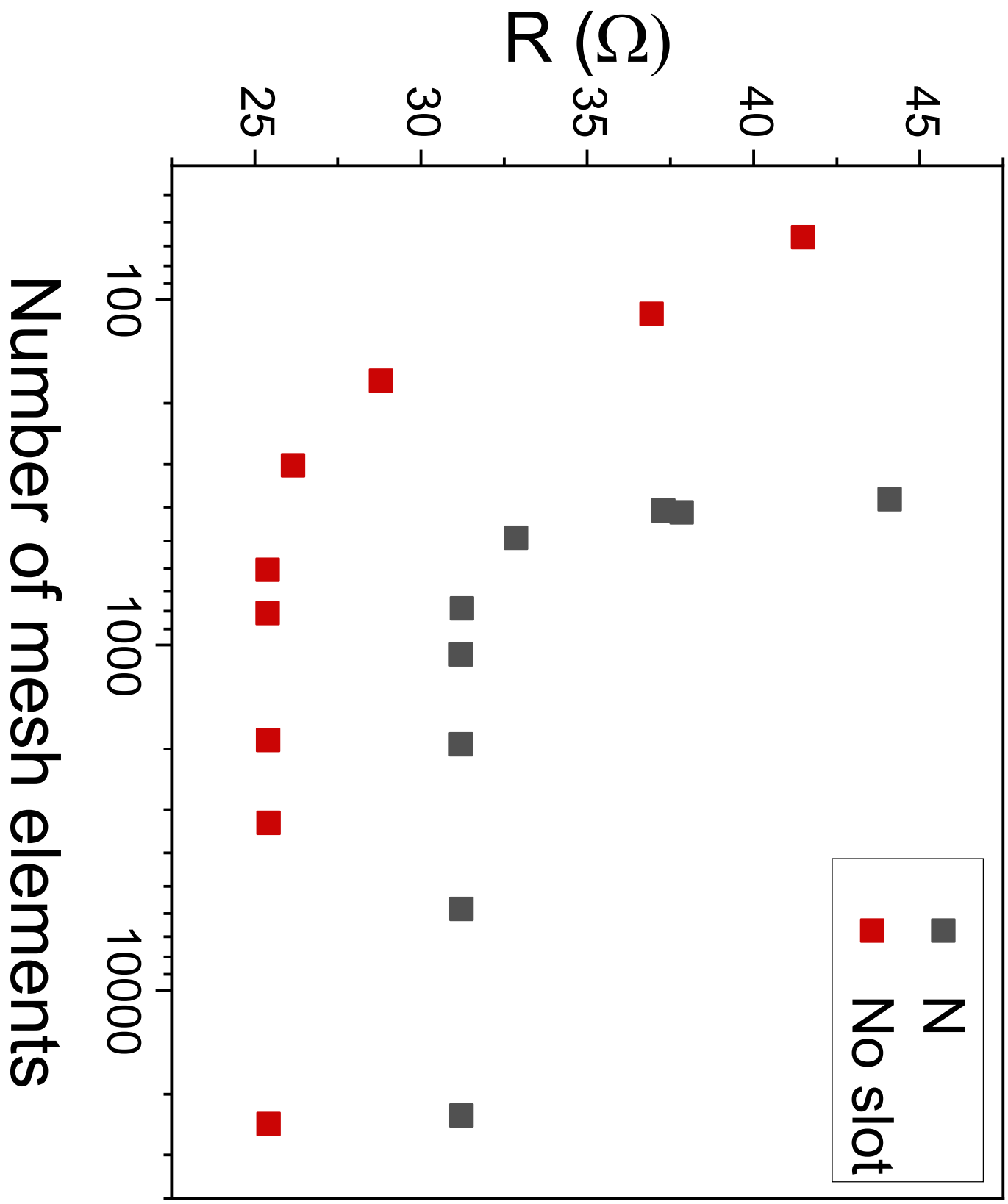

AIP Publishing

Journal of Applied Physics

ACCEPTED MANUSCRIPT

This is the author's peer reviewed, accepted manuscript. However, the online version of record will be different from this version once it has been copyedited and typeset.
PLEASE CITE THIS ARTICLE AS DOI: 10.1063/5.0154997

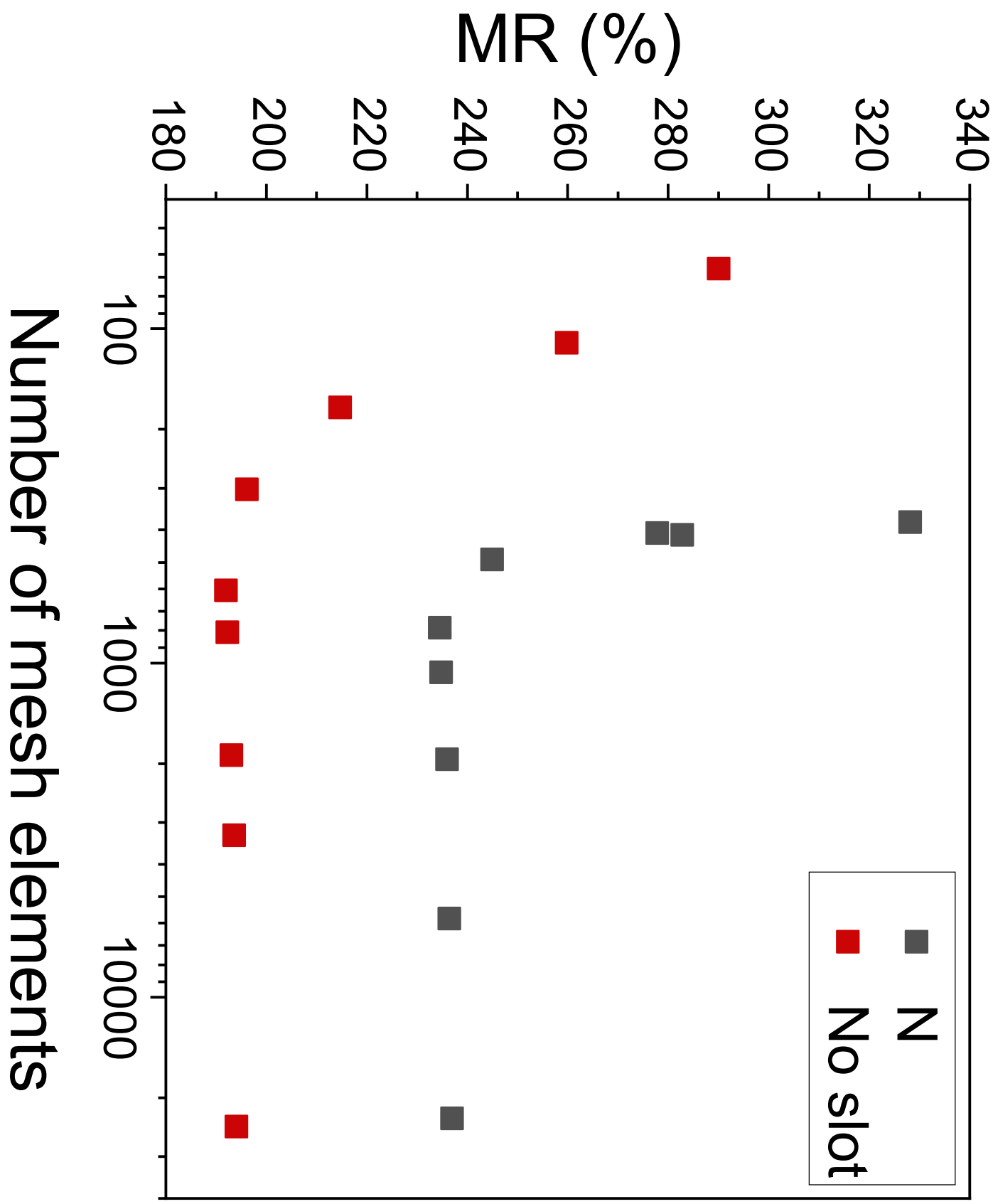

AIP Publishing

Journal of Applied Physics

ACCEPTED MANUSCRIPT

This is the author's peer reviewed, accepted manuscript. However, the online version of record will be different from this version once it has been copyedited and typeset.
PLEASE CITE THIS ARTICLE AS DOI: 10.1063/5.0154997

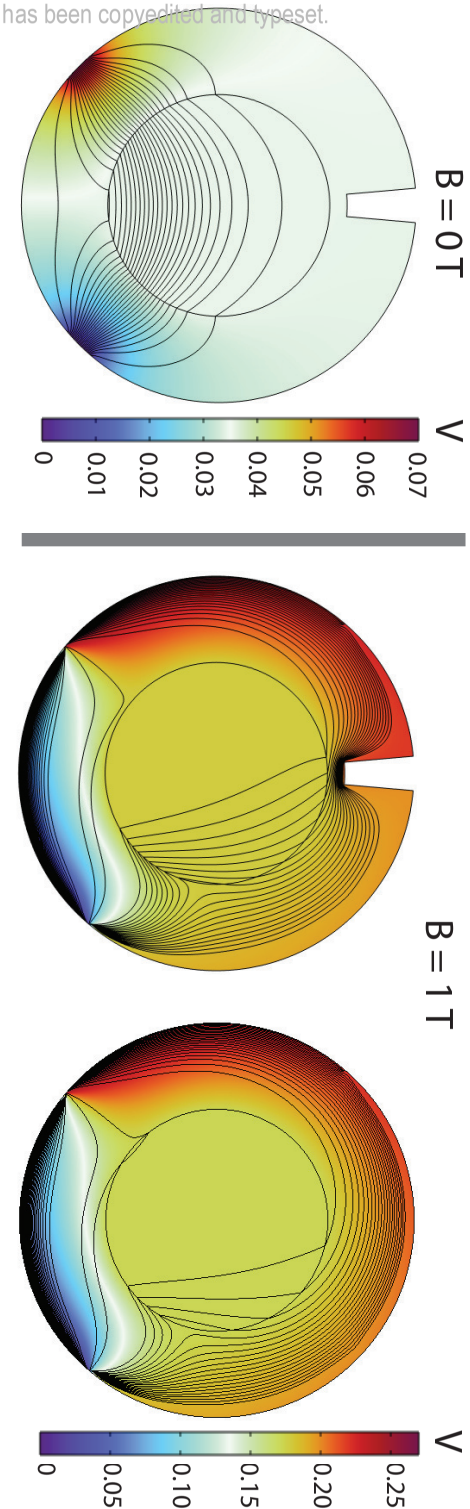

Journal of Applied Physics
AIP Publishing

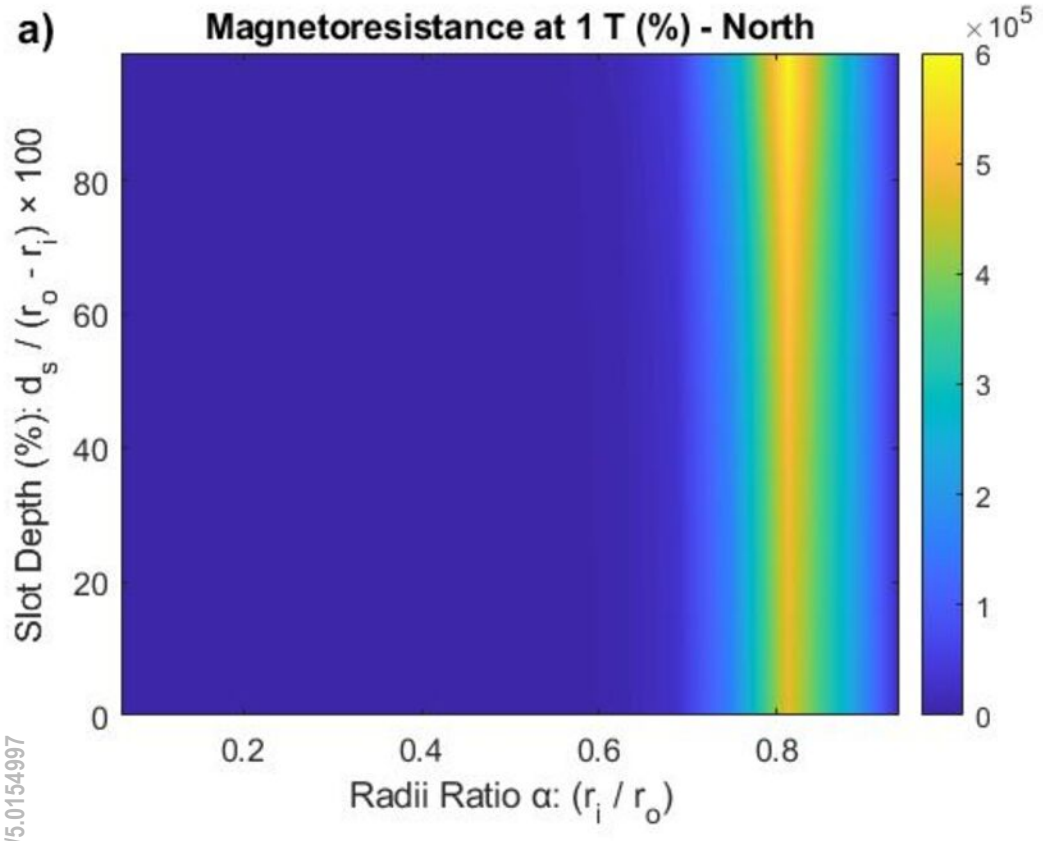

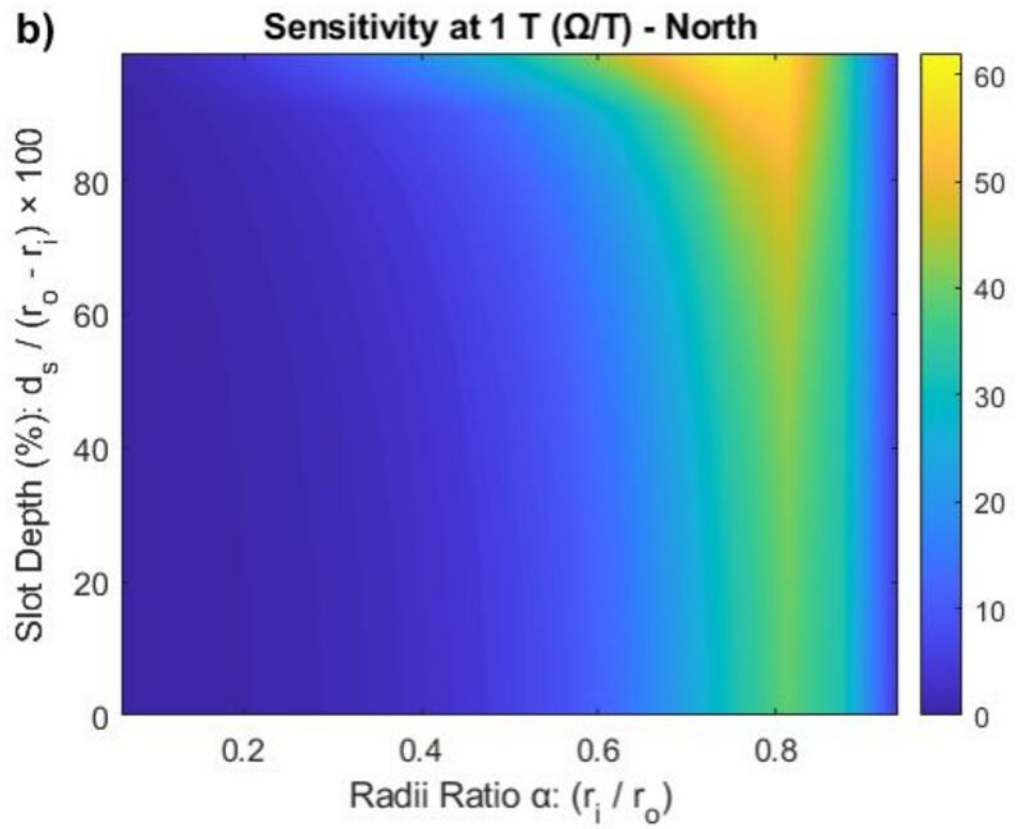

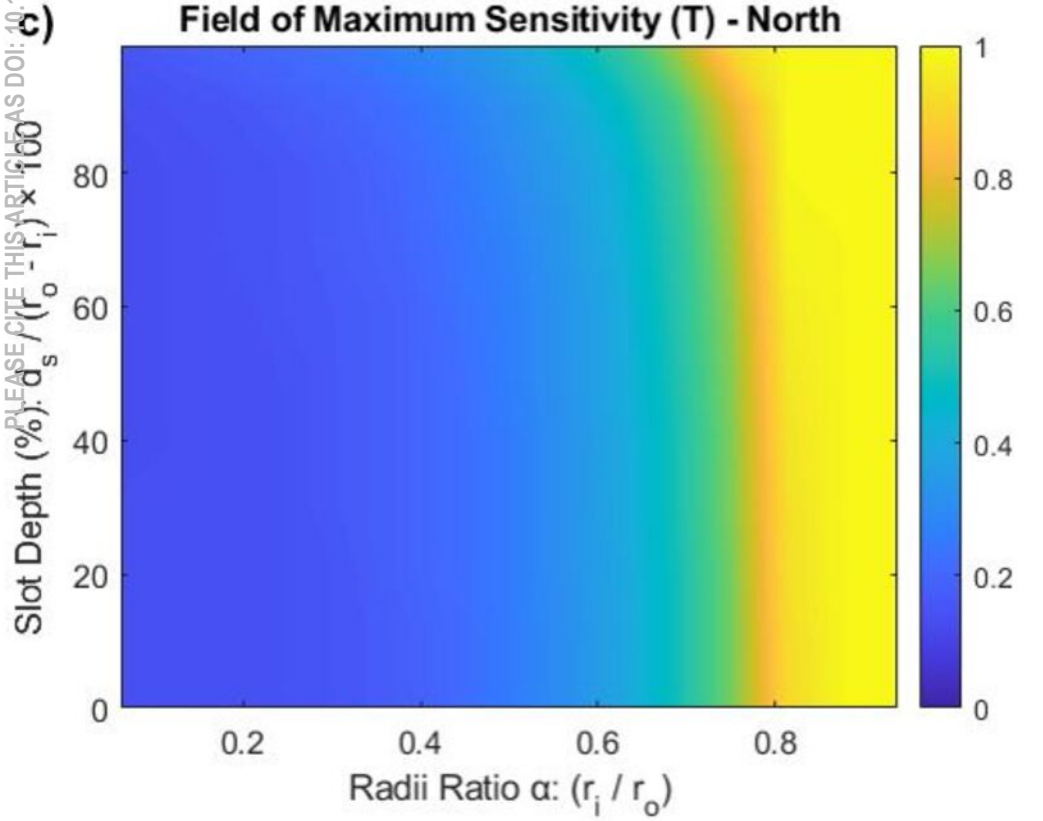

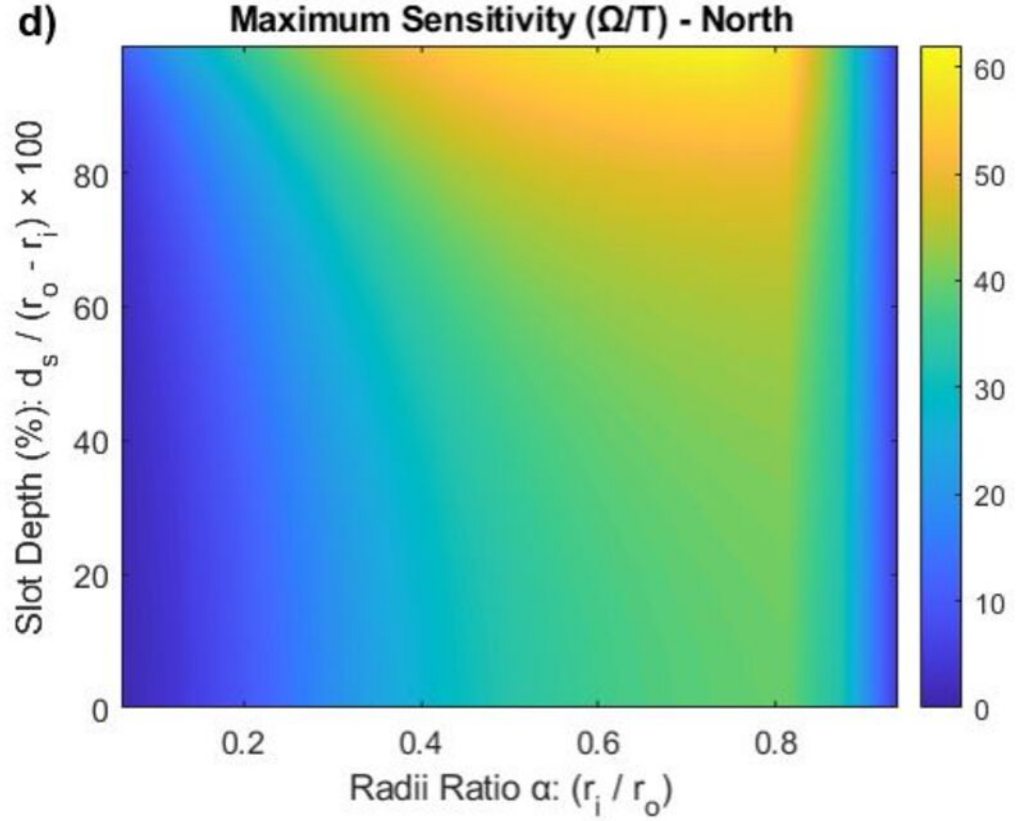

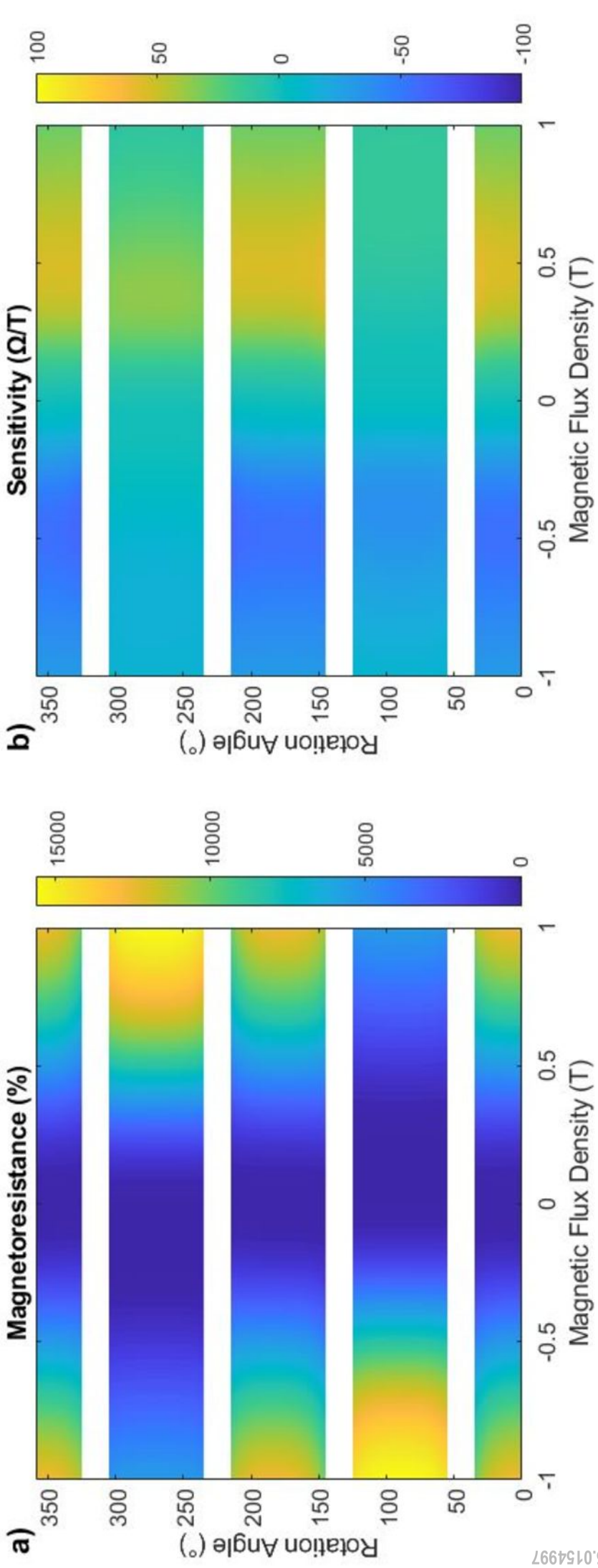

Journal of Applied Physics
AIP Publishing

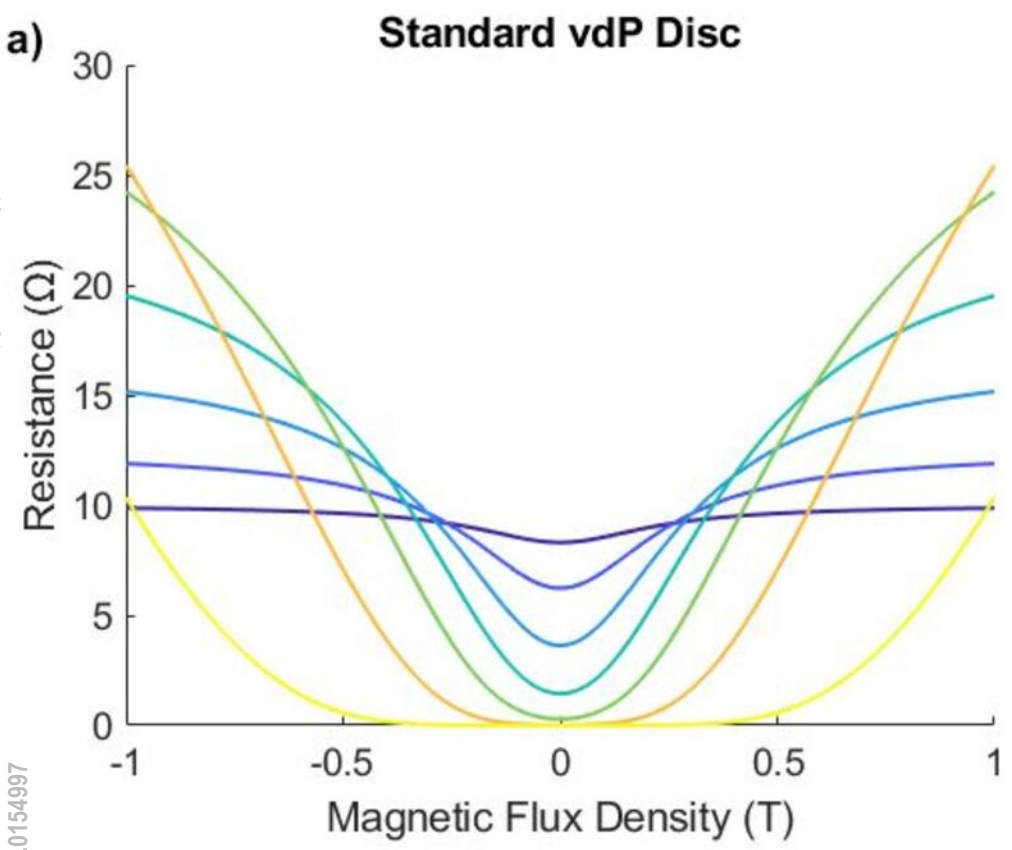

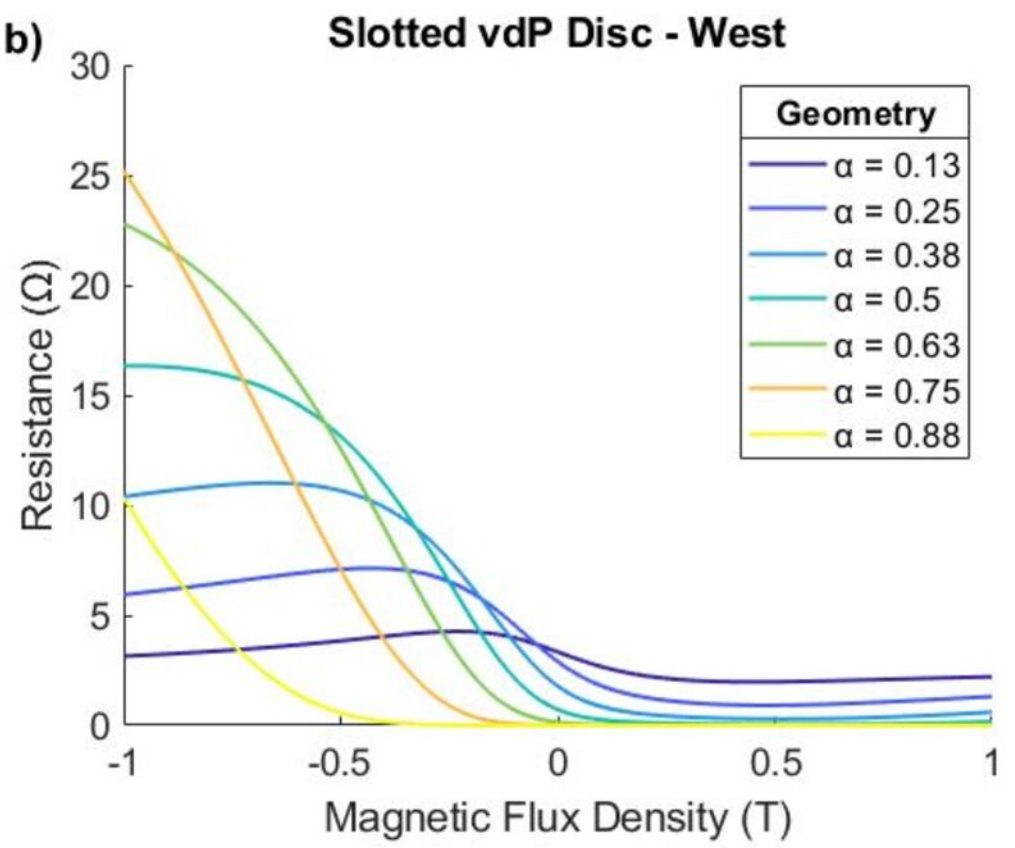

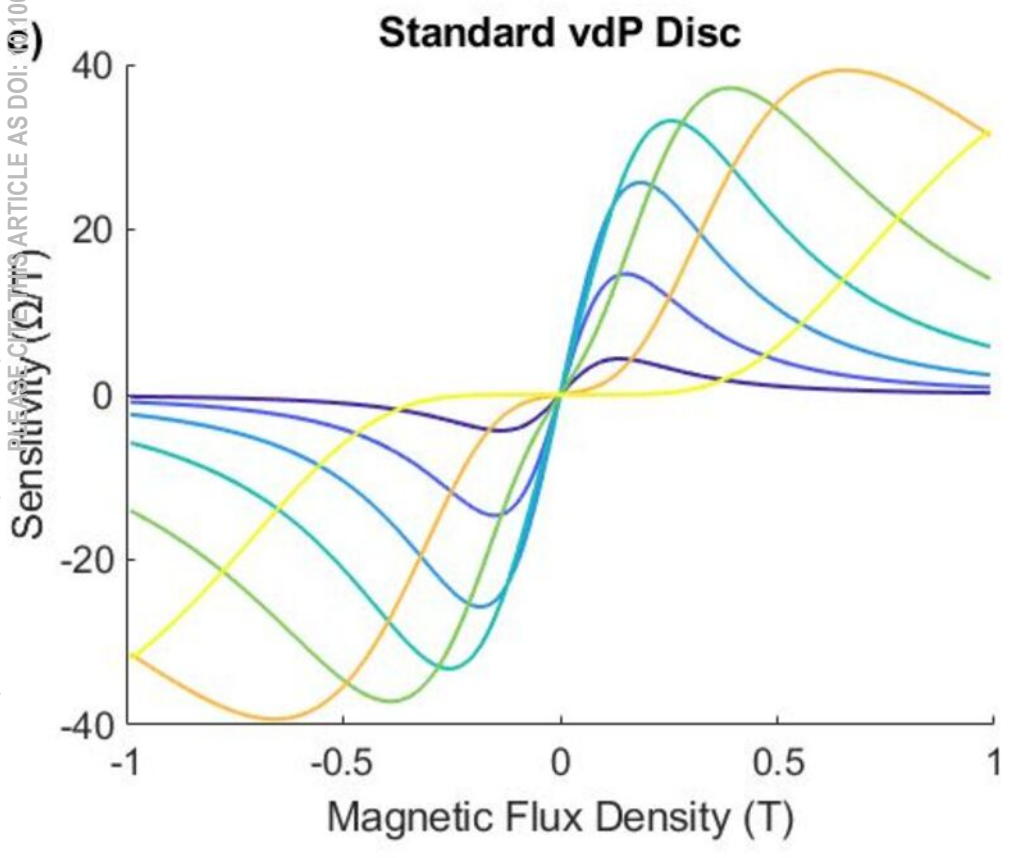

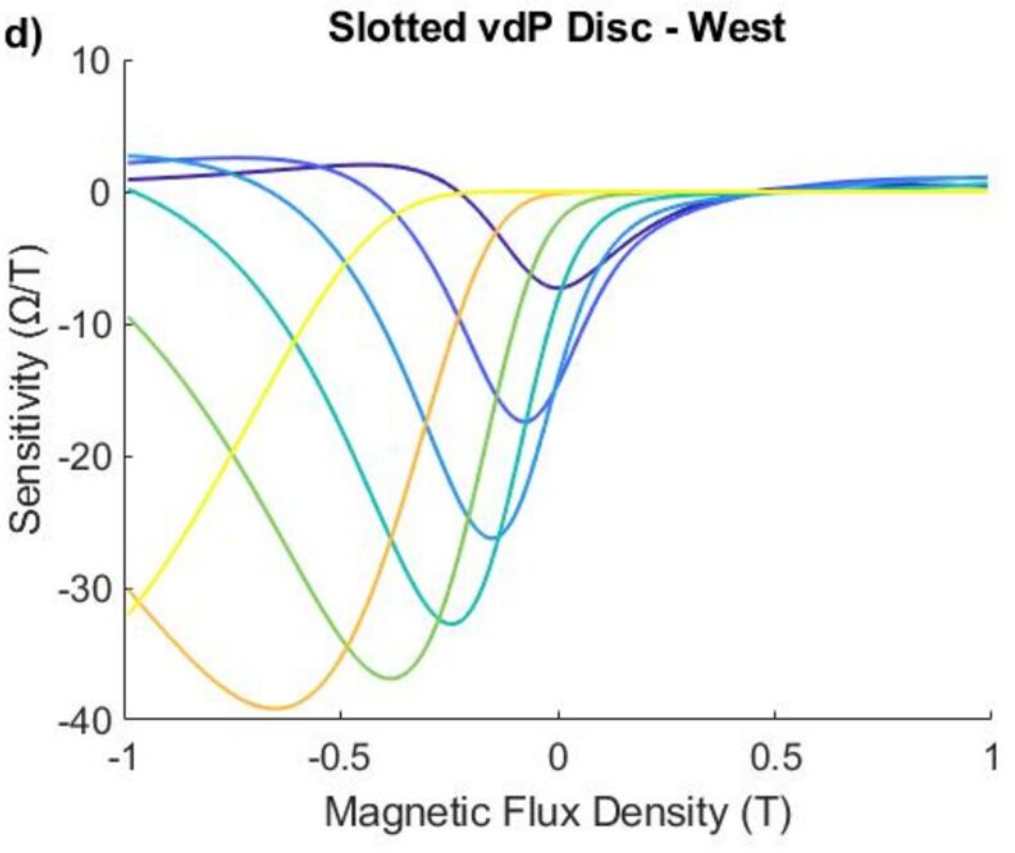

Journal of Applied Physics
AIP Publishing

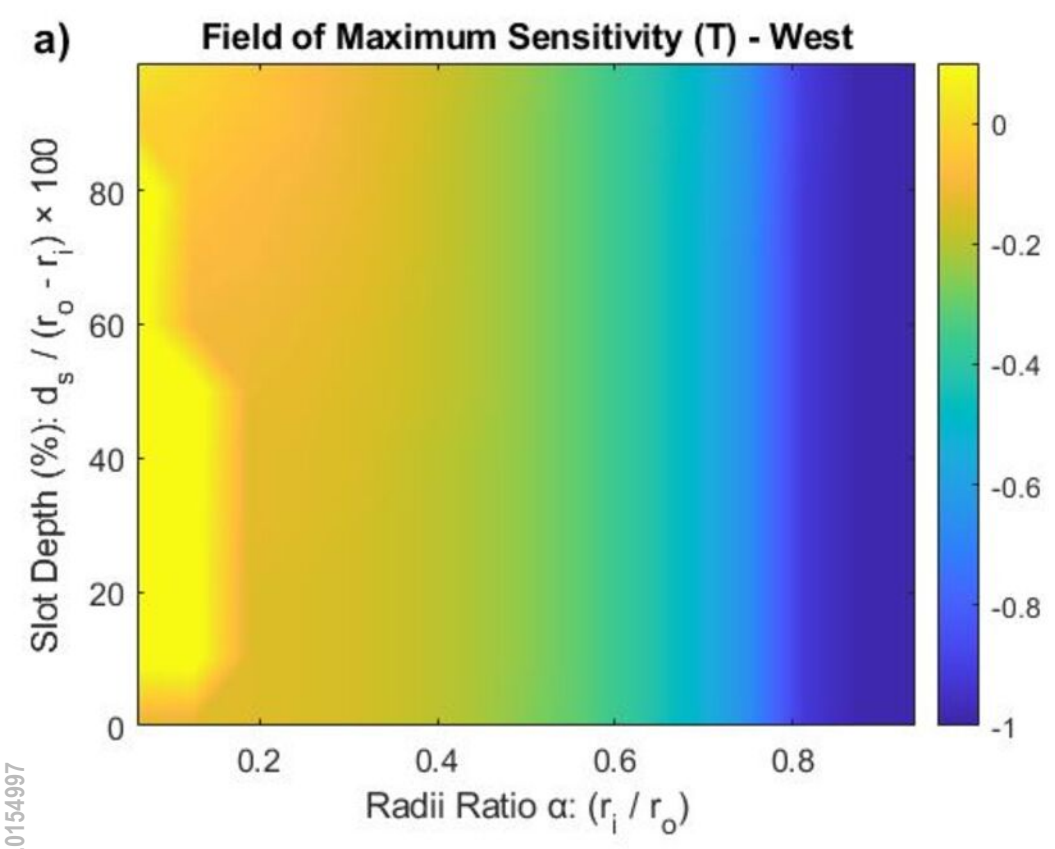

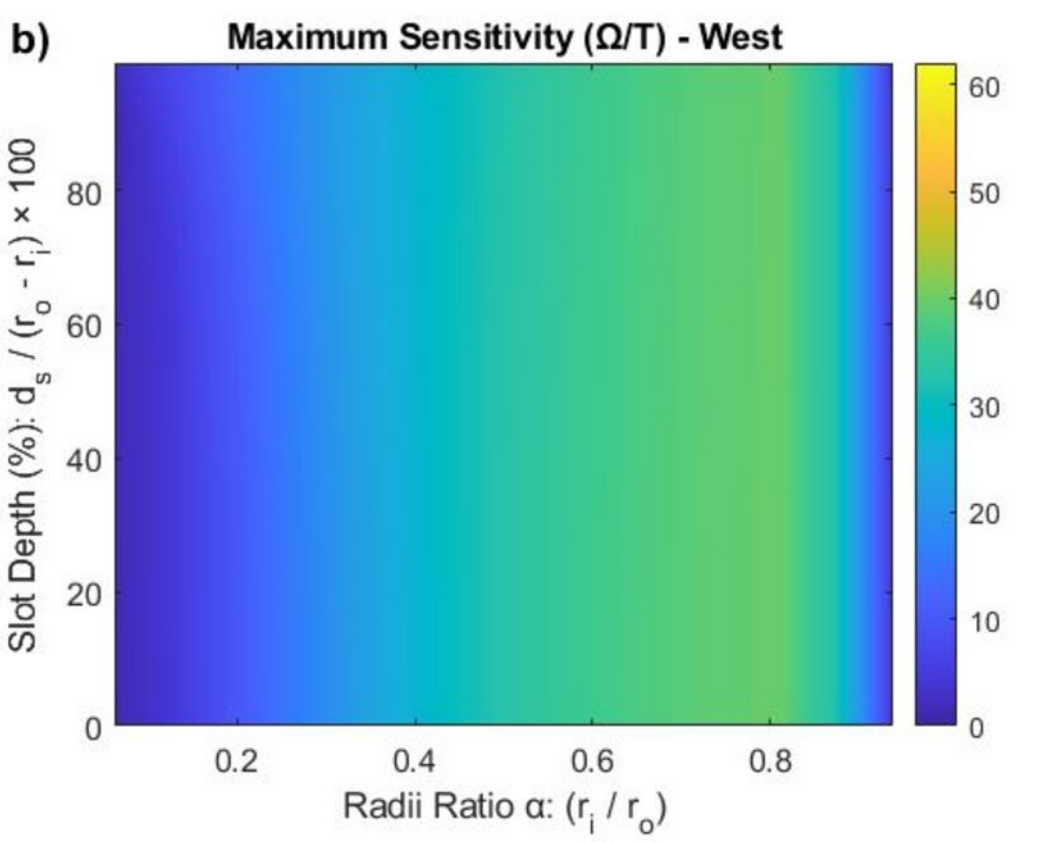

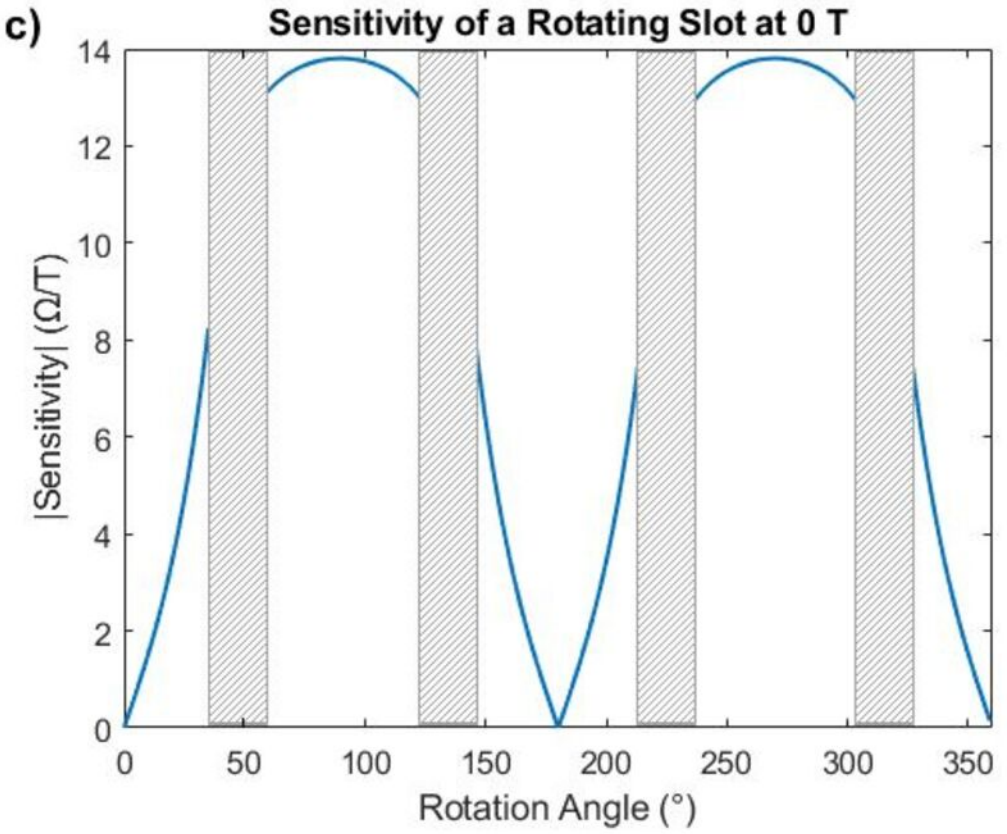

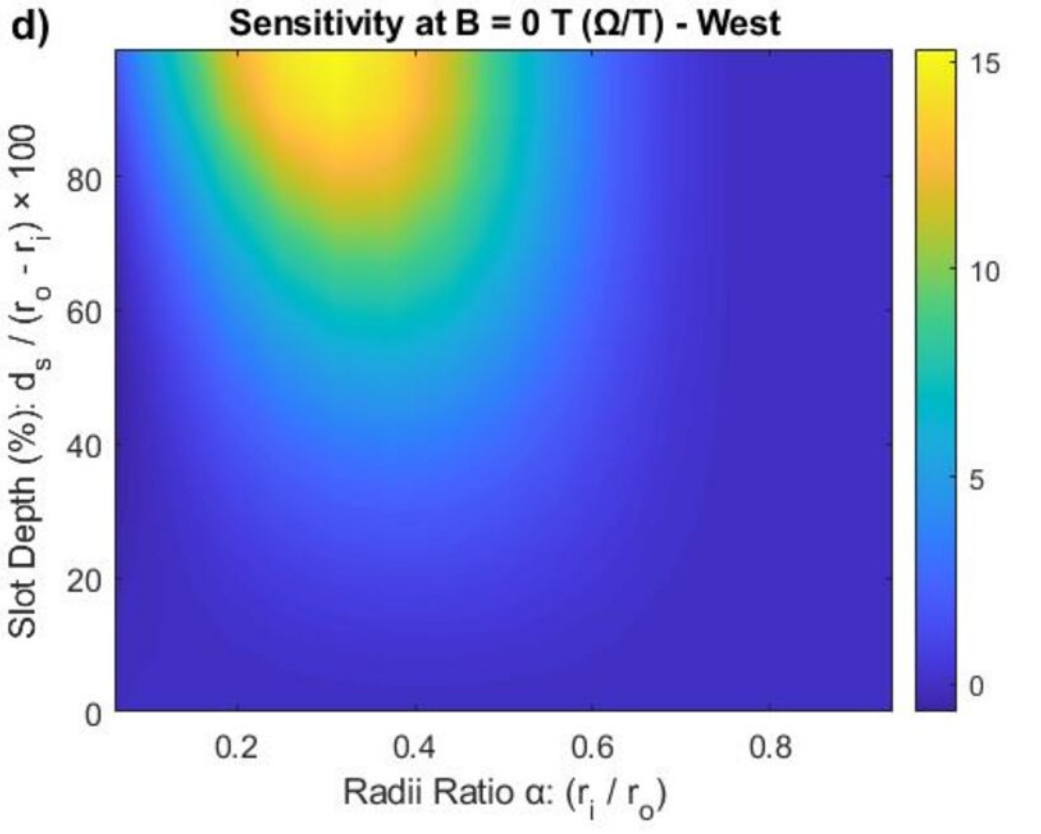

Journal of Applied Physics

AIP Publishing

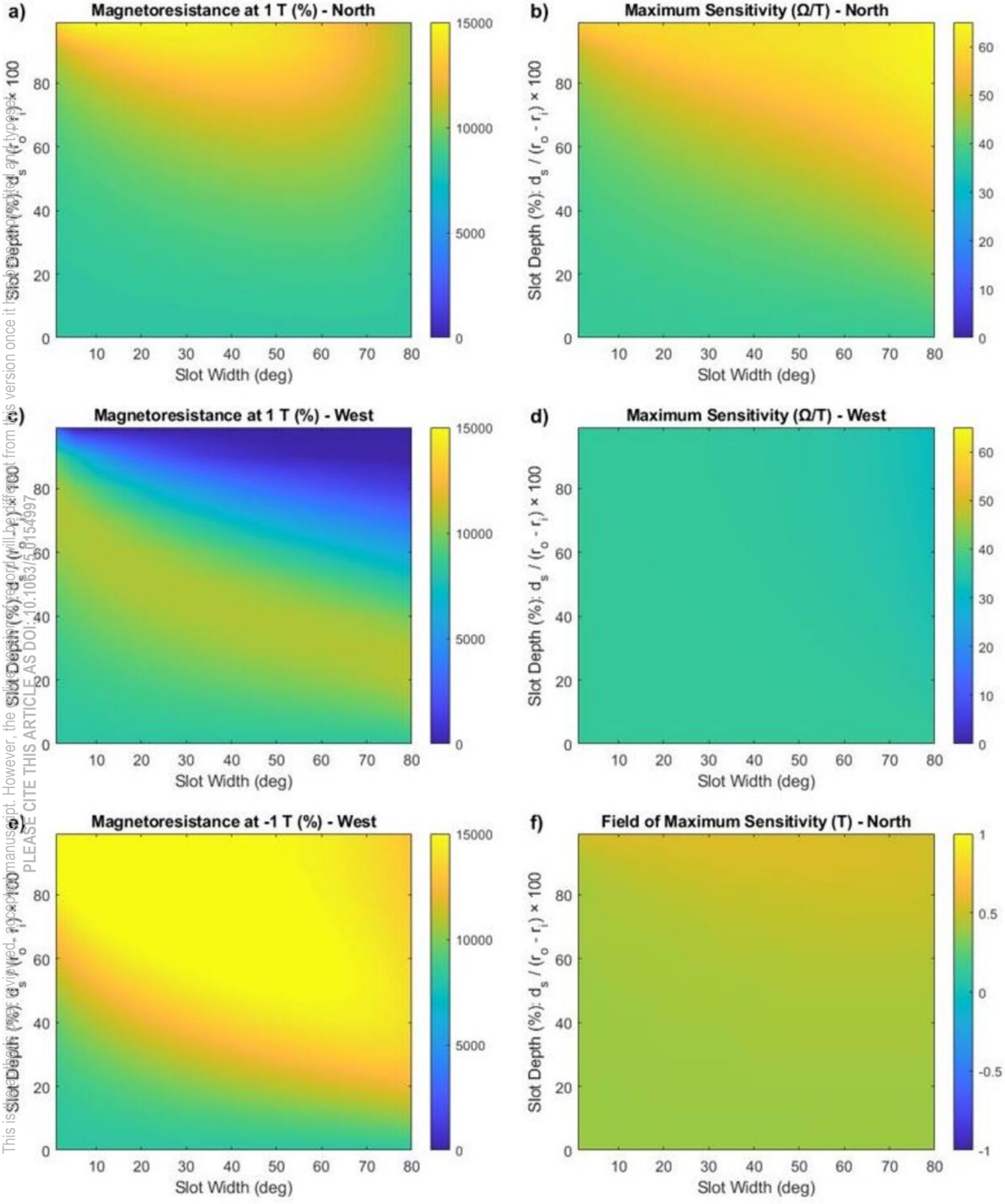

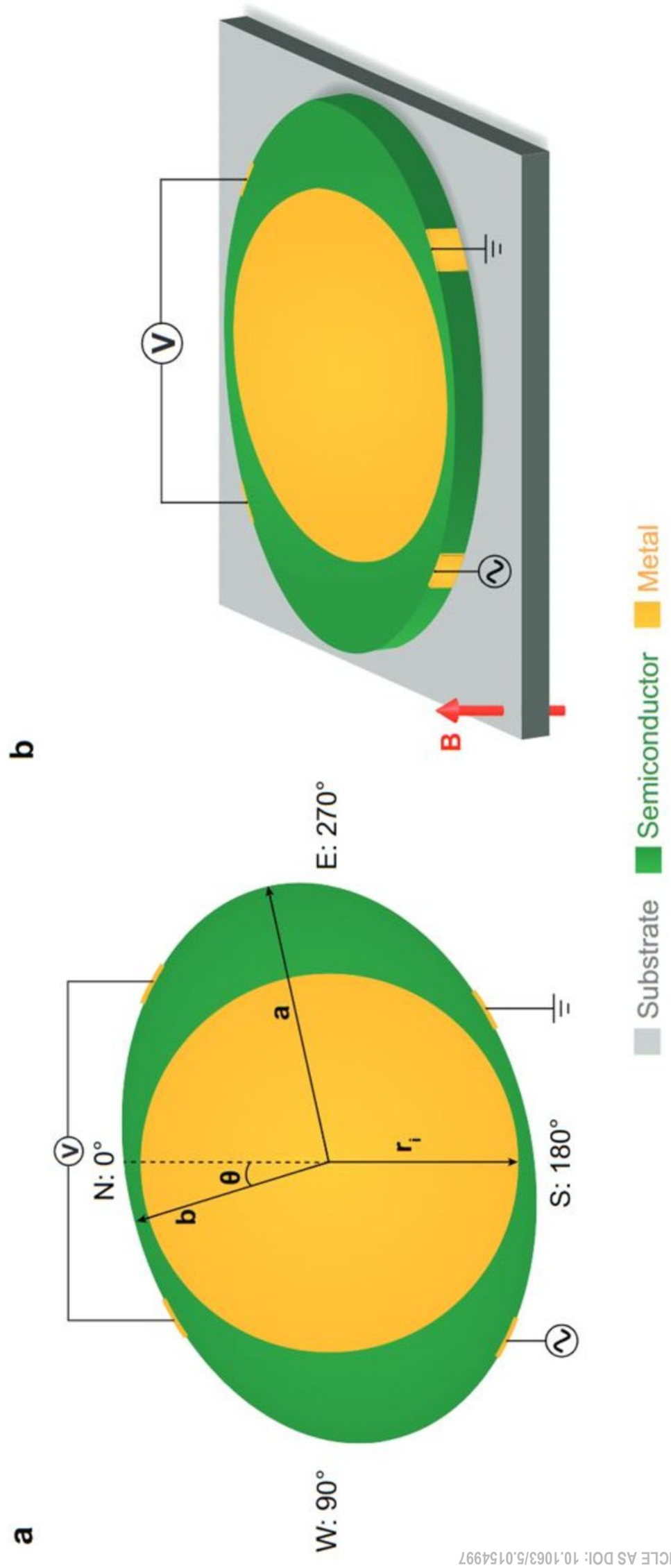

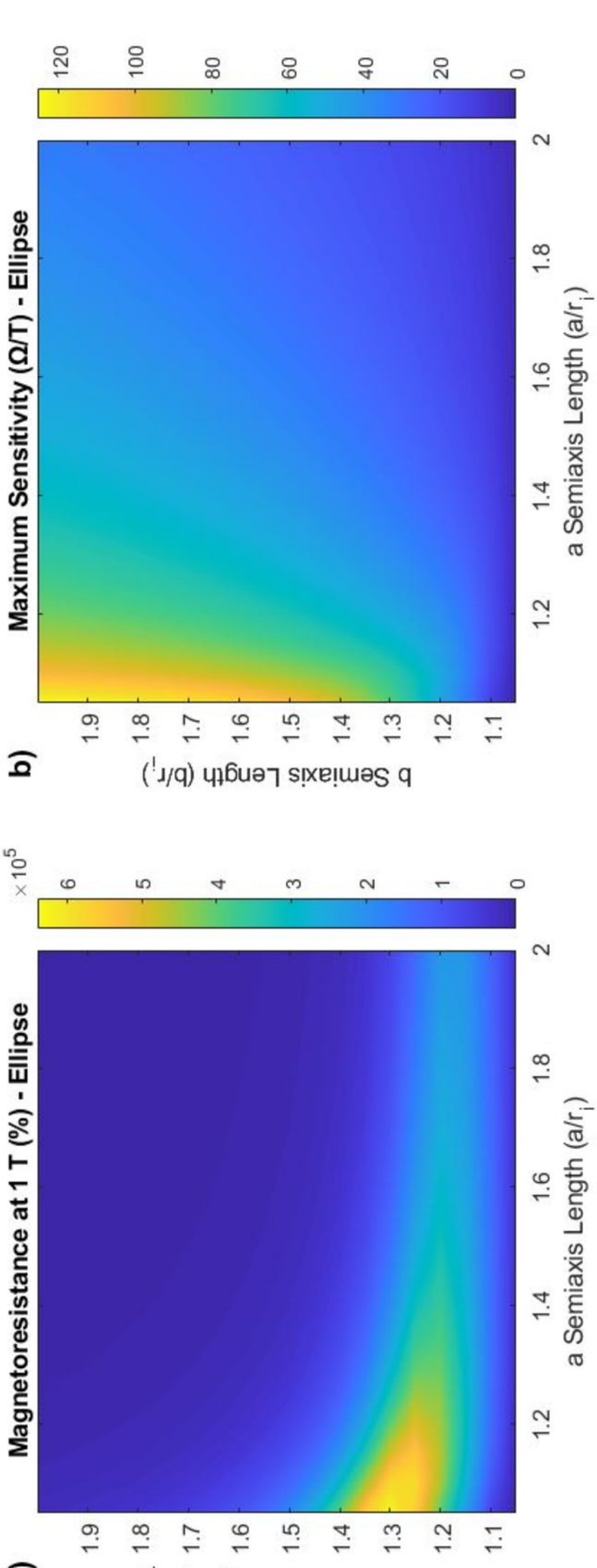

AIP Publishing

Journal of Applied Physics

ACCEPTED MANUSCRIPT

This is the author's peer reviewed, accepted manuscript. However, the online version of record will be different from this version once it has been copyedited and typeset.
PLEASE CITE THIS ARTICLE AS DOI: 10.1063/5.0154997

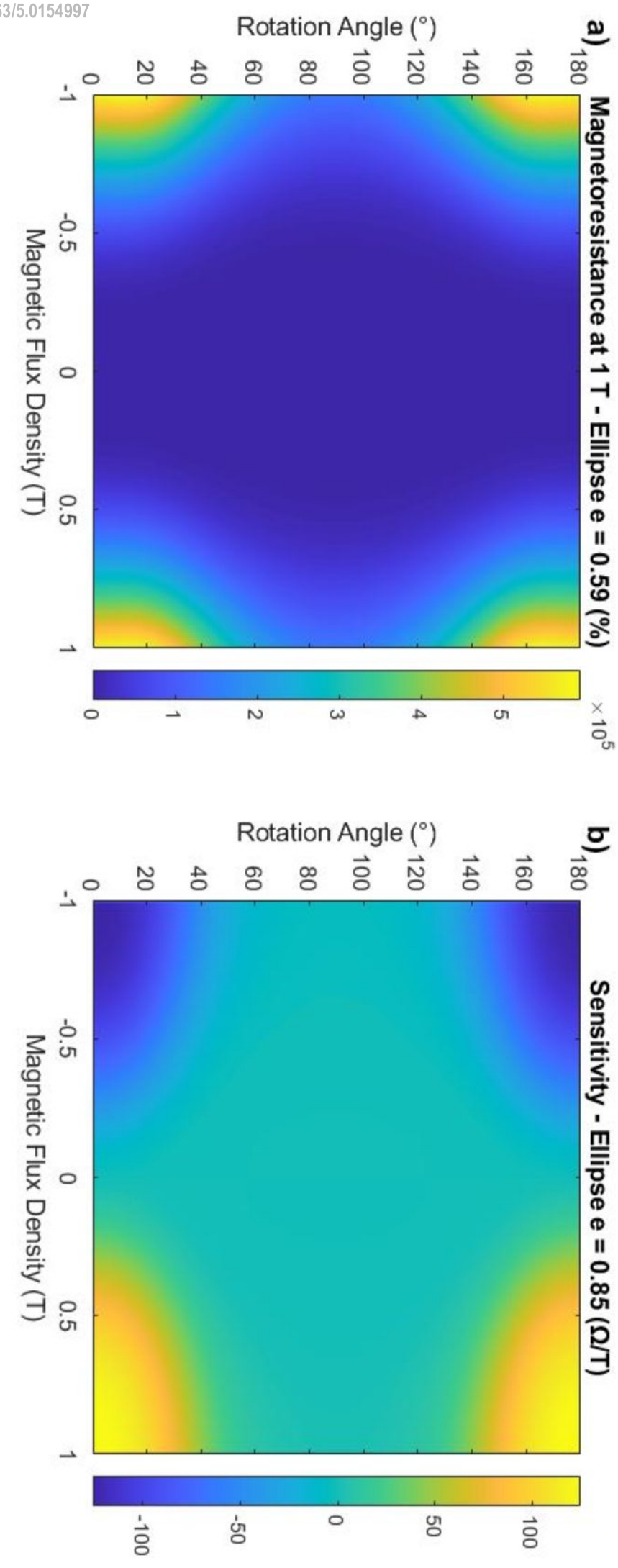

Journal of Applied Physics

AIP Publishing